A synthesis method for combined optimization of multiple antenna parameters and antenna pattern structure

Research Report
ISSN 0167-9708
Coden: TEUEDE

Eindhoven
University of Technology
Netherlands

Faculty of Electrical Engineering

A Synthesis Method for Combined Optimization of Multiple Antenna Parameters and Antenna Pattern Structure

by
P.J.I. de Maagt

EUT Report 90-E-246-X
ISBN 90-6144-246-X
November 1990

Eindhoven University of Technology Research Reports

EINDHOVEN UNIVERSITY OF TECHNOLOGY

Faculty of Electrical Engineering
Eindhoven The Netherlands

ISSN 0167-9708 Coden: TEUEDE

A SYNTHESIS METHOD FOR COMBINED OPTIMIZATION OF MULTIPLE ANTENNA PARAMETERS AND ANTENNA PATTERN STRUCTURE.

by
P.J.I. de Maagt

EUT Report 90-E-246
ISBN 9o-6144-246-X

EINDHOVEN
NOVEMBER 1990

CIP-GEGEVENS KONINKLIJKE BIBLIOTHEEK, DEN HAAG

Maagt, P.J.I. de

A synthesis method for combined optimization of multiple antenna parameters and antenna pattern structure / by P.J.I. de Maagt. - Eindhoven: Eindhoven University of Technology, Faculty of Electrical Engineering. - Fig., tab. - (EUT report, ISSN 0167-9708; 90-E-246)
Met lit. opg., reg.
ISBN 90-6144-246-X
SISO 666.2 UDC 621.396.677.833 NUGI 832
Trefw.: reflectorantennes.

Abstract

This report deals with an analytical approach of antenna synthesis. It presents a optimization method which is based on writing the design criteria as a ratio of two quadratic Hermitian forms, so that more than one antenna parameter (such as antenna efficiency and beam efficiency) can be optimized simultaneously, with and without pattern–structure constraints.

Firstly the mathematical formulation is given; then the optimization method is discussed with and without constraints to the far–field pattern. Finally, a comparison is made with the results obtained by others and examples are given. This clearly shows the capability and correctness of the optimization procedure.

Maagt, P.J.I. de
A SYNTHESIS METHOD FOR COMBINED OPTIMIZATION OF MULTIPLE ANTENNA PARAMETERS AND ANTENNA PATTERN STRUCTURE.
Faculty of Electrical Engineering, Eindhoven University of Technology, The Netherlands, 1990.
EUT Report 90-E-246

Address of the author:

Ir. P.J.I. de Maagt,
Telecommunications Division,
Faculty of Electrical Engineering,
Eindhoven University of Technology,
P.O. Box 513,
5600 MB EINDHOVEN,
The Netherlands

Acknowledgements

Firstly, I wish to express my thanks to prof.dr.ir G. Brussaard and dr.ir. M.H.A.J. Herben for their guidance and invaluable comments.

Furthermore, credit goes to some members of the mathematical department, especially, prof.dr.ir J. Boersma for the help with the special functions, ir. C.J.J.M. van Ginneken for helping to choose the best software, and dr.ir. H.G. ter Morsche for the interesting discussions.

Finally, I want to thank dr. P.R. Attwood for reading and correcting the grammar of the original version of this report.

Table of contents

1 Introduction

Generally speaking, the objective of antenna synthesis is to reach the best possible design under the condition that requirements with respect to radiation properties are met. Synthesis techniques can be divided into two categories. In one category, the solution is found via numerical manipulations; while in the other, the solution is found analytically. The latter has the advantage that it offers more insight into the effects and interactions between different design parameters. Furthermore, that method gives a closed form to both the aperture–field distribution and the far–field pattern. After optimization, the far–field will be known across the full angle–region of interest, which removes the need to compute the time consuming far–field integrals repeatedly.

The analytical method often uses the concept of partial radiation–patterns, and approximates the desired far–field pattern and the corresponding aperture–field distribution by means of a series of special source functions.

For the application of this method, two aspects require attention. Firstly, the selection of special functions can be governed by certain considerations, including: the simplicity of approximating the desired pattern with a minimum number of terms in a series, the property of orthogonality, the ease with which functions can be Fourier transformed or by the possibility of working with a series of functions with which one is familiar (some degree of arbitrariness can not be denied). Secondly and more demanding, is the aspect that "the requirements with respect to radiation properties" can vary widely and can often be mutually exclusive.

Due to these two aspects, a whole range of synthesis procedures exists. Most of them are focused on one specific design objective and are applied to earth–stations for satellite communications.

There are synthesis methods in which only the pattern shape is modified ([1],[2],[3]). Or optimization techniques without pattern constraints ([4], [5], [6], [7], [8], [9]). Borgiotti [4] and Mironenko [5] discuss methods to maximize the fraction of power radiated in a prescribed solid angle, while Minkovich [6] and Yurjev [7] deal with problems in terms of maximum main lobe power and low sidelobe level or minimum total power of side lobe radiation. References [8] (Kouznetsov) and [9] (Sanzgiri) deal with sidelobe envelope. Some methods include constraints but optimize only one design objective ([10],[11],[12]). The constraints can be sidelobe peak level (Sanzgiri [10]) , pattern nulls (Drane [11]) or main lobe beam width (Kurth [12]).

It is clearly desirable that a more general technique could be used which has the possibility of dealing with many different design criteria.
If possible this method should deal with design criteria:

- irrespective of the source functions used
- separately and with a set of design criteria at the same time
- with and without pattern constraints
- with and without blockage
- with and without ϕ–dependence.

The technique described in this report is pleasingly elegant if optimization problems are concerned. Even optimization problems with constraints can be solved simply. Most engineers turn to Lagrange multipliers if constraints are included. However, due to the elegant form, it appears to be possible to simplify the problem. In the proposed optimization method the constraints are treated as a "benefit" because they reduce the number of variables which can be adjusted.

In section 2 some antenna parameters (such as antenna efficiency, beam efficiency, or the normalized second moment) are fitted into a suitable form and in section 3 it is shown that optimization problems reduce to simple problems which can be solved with basic theorems from linear algebra.

In section 4 different source functions are introduced and optimization examples are given. Numerical results are given in several tables. In section 5 the different source functions are compared.

Cross–polar synthesis and blocked aperture distributions are treated in sections 6 and 7, respectively.

No attempt has been made to include in this treatise all of the results that have been published by others on the problem of synthesis. Therefore, a selection has been made. This selection intends to reach a large variety of source functions adopted and pattern requirements stated.

2 Writing antenna parameters in a suited form

In this section it is shown that a variety of antenna parameters (such as antenna efficiency, beam efficiency, normalized second moment, etc) can be written in a particular, suited form. The starting point is a circular aperture located in the x–y plane as shown in figure 2.1.,

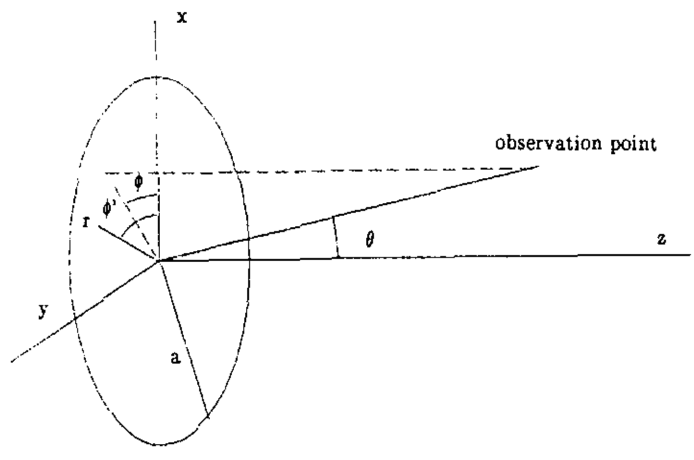

Figure 2.1 Coordinate system.

The aperture points are given by normalized aperture polar coordinates (r,ϕ') and the far field observation point by spherical coordinates (R,θ,ϕ). The integral part g(u,ϕ) of the far field pattern E(R,θ,ϕ) [13] is related to the aperture distribution f(r,ϕ') by the integral [13]:

$$g(u,\phi) = a^2 \int_0^{2\pi} \int_0^1 f(r,\phi')\, e^{jur\cos(\phi-\phi')}\, r dr d\phi' \tag{2.1}$$

with $u = \frac{2\pi a}{\lambda} \sin\theta = \frac{\pi D}{\lambda} \sin\theta$

When f(r) is a ϕ–independent, uniform–phase aperture distribution, g(u) can be written as the first order Hankel transform :

$$g(u) = 2\pi a^2 \int_0^1 f(r)\, J_0(ur)\, rdr \qquad (2.2)$$

If f(r) is written as:

$$f(r) = \begin{cases} \sum_{n=0}^{N} a_n e_n(r) & 0 \leq r \leq 1 \\ 0 & \text{elsewhere} \end{cases} \qquad (2.3)$$

where a_n are the excitation coefficients of the elementary real functions $e_n(r)$ and J_0 is the Besselfunction of the first kind and zeroth order, it is possible to split the Hankel transform into a set of integrals as follows:

$$g(u) = 2\pi a^2 \sum_{n=0}^{N} a_n I_n(u) = 2\pi a^2 \sum_{n=0}^{N} a_n \int_0^1 e_n(r)\, J_0(ur)\, rdr \qquad (2.4)$$

To derive the equations for the different antenna parameters, the equations for the power radiated by the aperture p_r, the power radiated within a prescribed solid angle $p_{r,angle}$, and the second moment μ_2 are needed. The first two are given by:

$$p_r = 2\pi a^2 \int_0^1 f^2(r)\, rdr \qquad p_{r,angle} = 2\pi \int_0^c u\, p(u)\, du \qquad (2.5)$$

with $p(u) = g^2(u)$ and $c = \frac{\pi D \sin \theta_{pre}}{\lambda}$, where θ_{pre} is the prescribed angle.

The second moment of the far field radiated power with respect to the axis u=0 is found by integrating $u^2 p(u)$. This leads to:

$$\mu_2 = \int_0^{\pi D/\lambda} u^2\, p(u)\, u\, du = \int_0^{\pi D/\lambda} u^3\, p(u)\, du \qquad (2.6)$$

The normalized second moment $\sigma^2 = \frac{\mu_2}{p_r}$ is a measure of the spread of the radiated power from the beam axis.

Some basic antenna definitions can now be written as:

aperture efficiency $$\eta_a = \frac{2\,p(0)}{p_r} \qquad (2.7)$$

beam efficiency $$\eta_b = \frac{p_{r,\,angle}}{p_r} \qquad (2.8)$$

normalized second moment $$\sigma^2 = \frac{\mu_2}{p_r} \qquad (2.9)$$

Using the equations (2.3) and (2.4), it is possible to write these antenna definitions into a form (known as the quotient of two Quadratic forms or Rayleigh quotient), which lends itself to evaluation with the help of basic theorems from linear algebra. To reach this, f(r), g(u) and p(u) are written as follows:

$$f(r) = \underline{a}^T \cdot \underline{e} \qquad 0 \leq r \leq 1 \qquad (2.10)$$
$$= 0 \qquad \text{elsewhere}$$

were $\underline{a}^T = (a_0, a_1, \ldots\ldots\ldots\ldots a_N)$ and $\underline{e}^T = (e_0, e_1, \ldots\ldots\ldots\ldots e_N)$,

$$g(u) = \underline{I}^T(e) \cdot \underline{a} \qquad (2.11)$$

with $\underline{I}^T(e)$ an N+1 element vector with elements:

$$I_i(e_i) = \int_0^1 e_i\, J_0(ur)\, r dr \qquad (i=0,\ldots.N), \qquad (2.12)$$

and,

$$p(u) = g^2(u) = \overline{g(u)}\,g(u) = \underline{a}^T \underline{I}(e) \underline{I}^T(e) \underline{a} = \underline{a}^T V \underline{a} \qquad (2.13)$$

with $V_{ij} = I(e_i)I(e_j)$ the elements of an N+1×N+1 element matrix V.

Using the above definitions, it is possible to describe the power radiated by the aperture and within a prescribed solid angle and the second moment in a comparable way:

$$p_r = \underline{a}^T A \underline{a} \tag{2.14}$$

with $A_{ij} = \int_0^1 e_i e_j \, r dr$ the elements of an N+1×N+1 element matrix A.

$$p_{r,angle} = \underline{a}^T X \underline{a} \tag{2.15}$$

with $X_{ij} = \int_0^c u \, V_{ij} \, du$ the elements of an N+1×N+1 element matrix X.

$$\mu_2 = \underline{a}^T W \underline{a} \tag{2.16}$$

with $W_{ij} = \int_0^{\pi D/\lambda} u^3 V_{ij} \, du$ the elements of an N+1×N+1 element matrix W.

The basic antenna definitions can now be expressed as a ratio of two quadratic forms:

$$\eta_a = \frac{2 \; \underline{a}^T V(0) \underline{a}}{\underline{a}^T A \underline{a}} \tag{2.17}$$

$$\eta_b = \frac{\underline{a}^T X \; \underline{a}}{\underline{a}^T A \underline{a}} \tag{2.18}$$

$$\sigma^2 = \frac{\underline{a}^T W \; \underline{a}}{\underline{a}^T A \underline{a}} \tag{2.19}$$

The matrices V,A,X,W have the property of being hermitian, because:

$$\aleph_{ij} = \overline{\aleph}_{ji} \quad \text{with } \aleph = V,A,X,W \tag{2.20}$$

where: $\overline{}$ denotes the complex conjugate.

This is immediately evident from equations (2.14)–(2.16). Furthermore, A ,X and W are positive definite because they represent the radiated power, the power radiated in a prescribed angle and the spread of radiated power, respectively.

3 The optimization procedure

3.1 Theorem

Consider the problem of maximizing a quantity which can be written as:

$$h(\underline{a}) = \frac{\underline{a}^T A \underline{a}}{\underline{a}^T B \underline{a}} \tag{3.1}$$

in which $\underline{a}$ is an N+1–element vector and A and B are N+1×N+1 real and square matrices. This form is known as a Rayleigh quotient, or quotient of two quadratic forms. The solution to the problem can be found in a basic theorem from linear algebra [14]. The theorem states that with A and B hermitian and B positive definite, the maximum (or minimum) of the quantity is given by the largest (or smallest) eigenvalue determined by:

$$A\underline{a} = \lambda B\underline{a} \tag{3.2}$$

So, the original problem can be treated as a general eigenvalue problem. The proof of this theorem can be deduced from the formula for the derivative of a vector–valued function in an N+1–dimensional space.

$$h(\underline{a}+\underline{h}) = h(\underline{a}) + J\underline{h} + \mathcal{O}(\underline{h}) \tag{3.3}$$

were J is the Jacobian matrix.

$$h(\underline{a}+\underline{h}) = \frac{\underline{a}^T A \underline{a} + 2\underline{h}^T A \underline{a} + \underline{h}^T A \underline{h}}{\underline{a}^T B \underline{a} + 2\underline{h}^T B \underline{a} + \underline{h}^T B \underline{h}}$$

$$= \frac{\underline{a}^T A \underline{a}}{\underline{a}^T B \underline{a}} \cdot \frac{1 + \dfrac{2\underline{h}^T A \underline{a}}{\underline{a}^T A \underline{a}} + \dfrac{\underline{h}^T A \underline{h}}{\underline{a}^T A \underline{a}}}{1 + \dfrac{2\underline{h}^T B \underline{a}}{\underline{a}^T B \underline{a}} + \dfrac{\underline{h}^T B \underline{h}}{\underline{a}^T B \underline{a}}}$$

$$= \frac{\underline{a}^T A \underline{a}}{\underline{a}^T B \underline{a}} \left(1 + \frac{2\underline{h}^T A \underline{a}}{\underline{a}^T A \underline{a}} - \frac{2\underline{h}^T B \underline{a}}{\underline{a}^T B \underline{a}} + \mathcal{O}(\underline{h}^2) \right)$$

neglecting $\mathcal{O}(\underline{h}^2)$ we get:

$$h(\underline{a}+\underline{h}) = \frac{\underline{a}^T A \underline{a}}{\underline{a}^T B \underline{a}} + \frac{2}{\underline{a}^T B \underline{a}} \underline{h}^T \left(A\underline{a} - \frac{B \underline{a}\, \underline{a}^T A \underline{a}}{\underline{a}^T B \underline{a}} \right) \tag{3.4}$$

in an extreme the following holds:

$$J\underline{h} = h(\underline{a}+\underline{h}) - h(\underline{a}) = 0$$

$$\Longrightarrow A\underline{a} - \left(\frac{\underline{a}^T A \underline{a}}{\underline{a}^T B \underline{a}}\right) B\underline{a} = 0 \Longrightarrow A\underline{a} = \lambda B\underline{a} \tag{3.5}$$

with $\lambda = \dfrac{\underline{a}^T A \underline{a}}{\underline{a}^T B \underline{a}}$

resulting in a generalized eigenvalue problem.

3.2 Some properties of generalized eigenvalue problems

Because the original problem can be treated as a generalized eigenvalue problem some properties, that can be used in the optimization, are summarized.

(1) Because B is non–singular the equations reduce to the standard eigenvalue problem form:

$$B^{-1}A\underline{a} = \lambda\underline{a} \tag{3.6}$$

(2) Because A and B are real and symmetric, the eigenvalues will be real.

(3) When A and B are real, symmetric and positive definite the eigenvalues will all be positive.

(4) Because A and B are both real and symmetric and B is positive definite, the equations may be transformed using the Choleski decomposition [31]:

$$B = LL^T \tag{3.7}$$

with L a lower triangular matrix. Multiplying equation (3.2) with L^{-1} gives:

$$L^{-1}AL^{-T}L^T\underline{a} = \lambda L^T\underline{a} \tag{3.8}$$

So λ are the eigenvalues of the symmetric matrix $L^{-1}AL^{-T}$ and the eigenvectors are $L^T\underline{a}$. A special case occurs when the matrix B is a rank 1 matrix, then only one eigenvalue is non–zero.

(5) When A and B are both diagonal matrices, the eigenvalues are :

$$\lambda_i = \frac{A_{i\,i}}{B_{i\,i}} \qquad (3.9)$$

and the eigenvectors are $(0,...0,a_i,0...0)$.

3.3 Constraints

The problem of optimizing a quantity subject to constraints is usually solved with the aid of Lagrange multipliers ([10],[11]).The Lagrange method is based on finding the so called Lagrange multipliers which form the best fit solution to the problem. This method states the problem as:

$\max f(\underline{a})|C\underline{a} = \underline{b} \Rightarrow \nabla\cdot f = C^T\lambda \wedge C\underline{a} = \underline{b}$. With C a M×N+1 constraint matrix (suppose there are M constraints), λ the Lagrange multipliers and ∇ the gradient. Consequently this method starts with N+M+1 equations. However, due to the elegant mathematical form adopted here it is possible to convert this N+1+M problem into a N+1–M problem. In this way, reducing the manipulations needed to come to a solution when the number of constraints is increased. An explanation for this is that constraints reduce the number of variables which can be adjusted. It is clear that when the number of constraints increases the number of variables which can be adjusted decreases (there are N+1 elementary functions so there can be N constraints). So, from an optimizing point of view it is favourable to keep the number of constraints as low as possible. In contrast to a "best–fit solution" constraints are all satisfied when the latter method is used.

For antenna problems, constraints can be represented in the following way:

$$\underline{I}^T(u_m)\cdot\underline{a} = v_{pre}\underline{I}^T(0)\cdot\underline{a} \Rightarrow (\underline{I}^T(u_m) - v_{pre}\underline{I}^T(0))\cdot\underline{a} = 0 \qquad (3.10)$$

where v_{pre} is the prescribed value in a point u_m relative to the value at $u = 0$. Or in a shortened notation:

$$\underline{a}^T \cdot \underline{q}_m = \underline{q}_m^T \cdot \underline{a} = 0 \tag{3.11}$$

with $\underline{q}_m$ the constraints vectors (m = 0,1,..,M < N+1).

The quantity to be optimized now becomes:

$$h(\underline{a}) = \frac{\underline{a}^T A \underline{a}}{\underline{a}^T B \underline{a}} \mid \underline{a}^T \underline{q}_m = 0 \quad (m = 0,1,...M \text{ and } M < N+1) \tag{3.12}$$

3.4 The optimization procedure with constraints

Suppose $\underline{q}_1, \underline{q}_2, ... \underline{q}_M$ span an M dimensional space $\mathscr{V}$ and the N+1–M dimensional space $\mathscr{V}^\perp$ is spanned by $\underline{w}_j$ (j = M+1,...N+1)

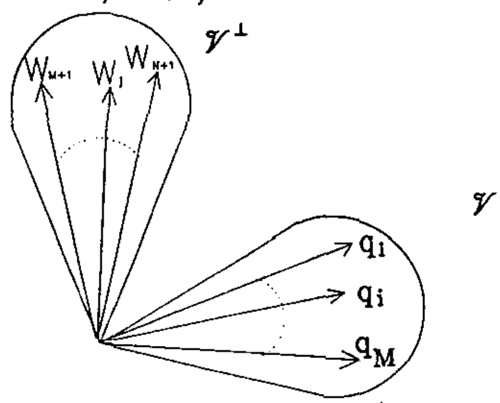

Figure 3.1 The space $\mathscr{V}$ and $\mathscr{V}^\perp$

Since $\underline{a}^T \underline{q}_m = 0$, the vector $\underline{a}$ must lie in $\mathscr{V}^\perp$ and it can be written as:

$$\underline{a} = \sum_{j=M+1}^{N+1} \underline{w}_j c_j = W\underline{c} \tag{3.13}$$

where $W = [\underline{w}_{M+1} | ..... | \underline{w}_{N+1}]$ is an N+1×N+1–M matrix (the columns are formed by the vectors $\underline{w}_j$) and $\underline{c}$ is an N+1–M vector. The problem has now been reduced to the determination of the vectors $\underline{c}$ and $\underline{w}_j$, and optimizing:

$$h(\underline{c}) = \frac{\underline{c}^T W^T A W \underline{c}}{\underline{c}^T W^T B W \underline{c}} \tag{3.14}$$

with W^TAW and W^TBW N+1–M×N+1–M real square matrices.

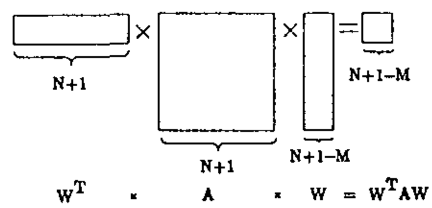

Figure 3.2 The product W^TAW

Finding a basis for $\mathcal{V}^{\perp}$ can be realized in different ways. One is via the Gram–Schmidt [31] transformation, but the Householder transform with partial pivoting [31] guarantees better numerical stability. A property of the Householder transform is that it reduces a N+1×M matrix $\mathcal{V}$($\mathcal{V}$= $[q_1 | q_2 | .... | q_M]$) to an upper tridiagonal form; with Q a N+1×N+1 orthogonal matrix (Householder matrix) and R an M×M upper tridiagonal matrix (see figure 3.3).

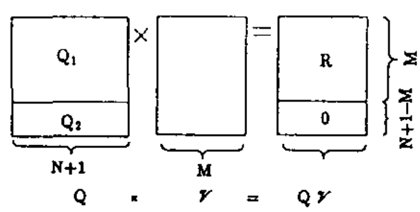

Figure 3.3 The product Q $\mathcal{V}$

Let Q be defined as:

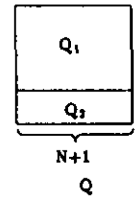

Figure 3.4 Q_1 and Q_2

Defining Q as stated above indicates that the last N+1–M rows of Q (=Q_2) form a basis for $\mathcal{V}^{\perp}$ (because $Q_2 \mathcal{V}= 0$). Substituting W = Q_2 in equation (3.14) gives:

$$h(\underline{c}) = \frac{\underline{c}^T Q_2^T A Q_2 \underline{c}}{\underline{c}^T Q_2^T B Q_2 \underline{c}} \tag{3.15}$$

The advantage of using the Householder transform now becomes clear, because the matrix product $Q_2^T A Q_2$ (or $Q_2^T B Q_2$) does not have to be evaluated by matrix multiplication, because it can be evaluated with two Householder transforms:

$$Q_2(Q_2A)^T \tag{3.16}$$

with Q_2A the last N+1−M rows of QA, $Q_2(Q_2A)^T$ the last N+1−M rows of $Q(Q_2A)^T$, thus forming a N+1−M×N+1−M square matrix. That the theorem for optimizing is still valid, might seem surprising at first sight. However the theorem is valid for both matrices Hermitian, and the matrix in the denominator positive definite. Now $(Q_2AQ_2^T)^T = Q_2A^TQ_2^T = Q_2AQ_2^T$ (A is Hermitian), making $Q_2AQ_2^T$ Hermitian. The same holds for $Q_2BQ_2^T$, so if $Q_2BQ_2^T$ is positive definite the theorem holds. This can easily be shown from the definition:

$Q_2BQ_2^T$ is positive definite if $\underline{x}^T Q_2BQ_2^T \underline{x} > 0 \ \forall \underline{x}$.

Let $Q_2^T x = y \Rightarrow y^T B y > 0$ (B is positive definite). This proofs that after deforming the N+1×N+1 problem into an N+1−M×N+1−M problem the theorem still holds.

It will be clear that the maximum (minimum) constrained eigenvalues $\lambda_{i,constr}$ will be smaller (greater) than the maximum (minimum) unconstrained λ_i.

Notice that, in the constrained case, we get a N−M element vector $\underline{c}$, when we started with an N element vector $\underline{a}$. The vector $\underline{a}$ can easily be calculated by using (3.13).

3.5 Optimizing a product of Quadratic forms

An interesting case will appear if more than one antenna parameter has to be optimized simultaneously. For a function which can be written as:

$$h_1(\underline{a})h_2(\underline{a}) = \frac{\underline{a}^T A \underline{a}}{\underline{a}^T B \underline{a}} \frac{\underline{a}^T C \underline{a}}{\underline{a}^T D \underline{a}} \tag{3.17}$$

its optimization can be solved with (see appendix 1) :

$$\left[\frac{1}{\underline{a}^T B \underline{a}} \frac{\underline{a}^T C \underline{a}}{\underline{a}^T D \underline{a}} A + \frac{1}{\underline{a}^T D \underline{a}} \frac{\underline{a}^T A \underline{a}}{\underline{a}^T B \underline{a}} C\right] \underline{a} = \tag{3.18}$$
$$= \lambda \left[\frac{1}{\underline{a}^T B \underline{a}} B + \frac{1}{\underline{a}^T D \underline{a}} D\right] \underline{a} \text{ or } E\underline{a} = \lambda\, F\underline{a}.$$

The proof of (3.18) can be deduced from the derivative of a vector–valued function in an N+1–dimensional space.

if B = D equation (3.18) reduces to :

$$\left[\frac{1}{2} \frac{\underline{a}^T C \underline{a}}{\underline{a}^T B \underline{a}} A + \frac{1}{2} \frac{\underline{a}^T A \underline{a}}{\underline{a}^T B \underline{a}} C\right] \underline{a} = \lambda\, B\underline{a} \quad \text{or } E'\underline{a} = \lambda\, F'\underline{a}. \tag{3.19}$$

The optimization is now done iteratively. A suitable vector $\underline{a}$ to start with is the eigenvector that corresponds to the largest eigenvalue of the two quadratic forms. After calculating the matrices E and F, a generalized eigenvalue problem of exactly the same form as that in (3.1) is obtained. The eigenvector corresponding to the optimum solution of $E\underline{a} = \lambda\, F\underline{a}$ is used in the next iteration. The computation can be continued until a maximum is reached with the desired degree of accuracy.

3.6 Maximum Sidelobes constraints

If there are requirements with respect to the sidelobe–peak levels within a specific angle region, the optimization procedure has to be done iteratively. Because the positions (u_m) of the peak levels are not known in advance, some starting positions have to be chosen. Suitable starting points will be those lying midway between the two nulls of the pattern in the unconstrained case. The starting points for any iteration step that follows will be midway between the old points and the position of the new maxima. This procedure is repeated till all sidelobe–peak levels have reached the desired level with a prescribed accuracy. If the problem requires the sidelobe envelope to be kept below a certain level, it is better to start the procedure with only one constraint with respect to that sidelobe which is closest to boresight that exceeds the prescribed sidelobe envelope (the first sidelobe). If the level of the next sidelobe away from boresight exceeds the prescribed level, the procedure has to be repeated with two constraints. This is done for all sidelobes within the angle region of interest. In this way, it is possible to end up with the highest number of variables which can be used for optimization purposes.

4. Various kinds of source functions

In this section various types of functions $e_n(r)$ are treated and some examples of optimization procedures (with or without constraints) are given.

4.1. Aperture distributions consisting of Besselfunctions

The first kind of aperture distribution which will be considered is the one using a series of Besselfunctions. Much of the work on optimization procedures involving Bessel functions has been reviewed by S.C.J. Worm [15]. For this case, f(r) can be written as:

$$f(r) = \begin{cases} \sum_{n=0}^{N} a_n J_0(\nu_n r) & 0 \leq r \leq 1 , \\ 0 & \text{elsewhere} \end{cases} \tag{4.1}$$

and g(u) can be calculated using Lommels Formula [16, p134],

$$\int_0^1 J_0(\nu_n r) J_0(ur) r dr = \frac{1}{u^2-\nu_n^2}\{uJ_0(\nu_n 1)J_0'(u1) - \nu_n J_0'(\nu_n 1)J_0(u1)\} \tag{4.2}$$

This gives for g(u):

$$g(u) = \sum_{n=0}^{N} \frac{a_n}{u^2-\nu_n^2} \{ uJ_0(\nu_n)J_0'(u) - \nu_n J_0'(\nu_n)J_0(u) \} \tag{4.3}$$

where J_0' denotes the derivative of J_0 with respect to r. The right hand side of equation (4.3) can be simplified through the choice of $J_0(\nu_n)$ or $J_0'(\nu_n) = 0$. Or more generally:

$$\nu_n J_0'(\nu_n) + hJ_0(\nu_n) = 0 \tag{4.4}$$

The case that h=0 (or $J_0'(\nu_n) = 0 \Longrightarrow J_1(\nu_n) = 0$) reduces to the Taylor distribution. The case h=∞ (or $J_0(\nu_n) = 0$) is a type of illumination which is investigated for

example by Kritsky [17].
Because the work of Taylor ([1],[18]) has had a profound influence on antenna synthesis, this distribution with $J_1(\nu_n) = 0$, will be considered first.

4.1.1 Aperture illumination $\sum_{n=0}^{N} a_n J_0(\nu_n r)$ with $J_1(\nu_n) = 0$

In this case, the aperture illumination consists of a series :

$$f(r) = \begin{cases} \sum_{n=0}^{N} a_n J_0(\nu_n r) & 0 \leq r \leq 1 \\ 0 & \text{elsewhere} \end{cases} \tag{4.5}$$

with $\nu_0 = 0$, $\nu_1 = 3.8317$,..........
Some functions $J_0(\nu_n r)$ are shown in figure 4.1.

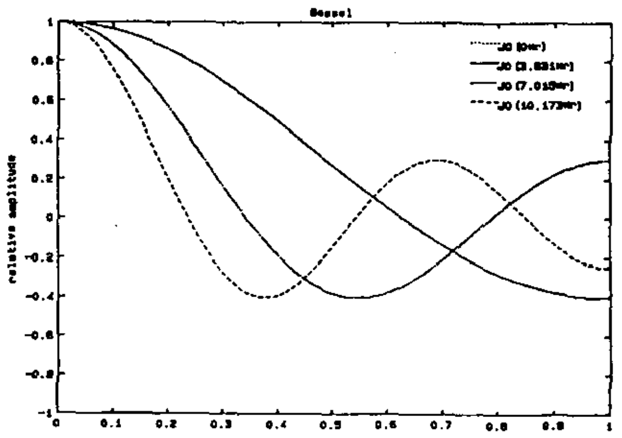

Figure 4.1 $J_0(\nu_n r)$ with $J_1(\nu_n) = 0$.

The far field is (for the case $J_1(\nu_n) = 0$, see (4.3)).

$$g(u) = \begin{cases} uJ_1(u) \sum_{n=0}^{N} \frac{a_n}{u^2-\nu_n^2} J_0(\nu_n) & \text{if } u \neq \nu_n \\ \frac{1}{2} a_n J_0^2(\nu_n) & \text{if } u = \nu_n \end{cases} \tag{4.6}$$

Fitting into the vector and/or matrix form gives:

$$\underline{e}^T = (1, J_0(\nu_1 r), \ldots\ldots\ldots\ldots J_0(\nu_N r)\ ) \tag{4.7}$$

$$\underline{I}^T(\underline{e}) = \frac{J_1(u)}{u}\left(1, \frac{u^2 J_0(\nu_1)}{u^2-\nu_1^2}, \ldots\ldots, \frac{u^2 J_0(\nu_N)}{u^2-\nu_N^2}\right) \tag{4.8}$$

Using Lommels equation [16, p134] gives :

$$A_{ij} = 0 \qquad \text{if } i \neq j \tag{4.9}$$
$$= \tfrac{1}{2} J_0^2(\nu_i) \qquad \text{if } i = j\,,$$

$$X_{ij} = J_0(\nu_i) J_0(\nu_j) \int_0^c \frac{u^3 J_1^2(u)}{(u^2-\nu_i^2)(u^2-\nu_j^2)} du\,, \tag{4.10}$$

$$W_{ij} = J_0(\nu_i) J_0(\nu_j) \int_0^{\pi D/\lambda} \frac{u^5 J_1^2(u)}{(u^2-\nu_i^2)(u^2-\nu_j^2)} du\,. \tag{4.11}$$

The elements of the matrices X and W given by equation (4.10) and (4.11) have to be calculated numerically.

Some examples

The unconstrained optimization of η_a can be done easily by making use of (3.9) which gives

$$\eta_{a,max} = 1 \tag{4.12}$$
$$\underline{a}^T = (1,0,\ldots\ldots,0) \tag{4.13}$$
$$g(u) = \frac{J_1(u)}{u} \tag{4.14}$$

Figure 4.2 gives the corresponding far field pattern and aperture distribution.

The unconstrained optimization of σ^2 and η_b is given in table A1 and A2, respectively (sll= sidelobelevel, u3dB = half of the 3 dB beamwidth). Tables which are referred to as A.xx are given in appendix 2. In this report the value c for the upper boundary of the integral of (2.5) has been taken as 3.5, unless otherwise specified. This value assures a narrow beam with a low first sidelobe [4], because it assures that even with an uniform illuminated aperture no sidelobe is in this region. Figure 4.3 shows some of the far field patterns for minimum σ^2 and the corresponding aperture distributions.

The unconstrained optimization of η_b gives the opportunity to compare the results with those in literature. Slepian [19] showed that the maximum of (2.10) is attained

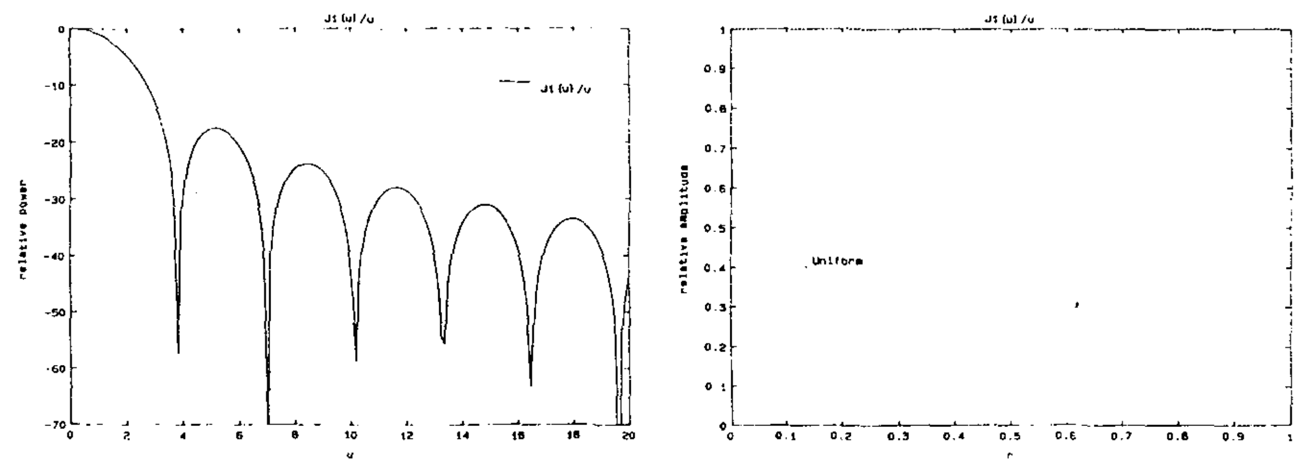

Figure 4.2 g(u) and f(r) for maximum η_a; using the series $\sum_{n=0}^{N} a_n J_0(\nu_n r)$ with $J_1(\nu_n) = 0$

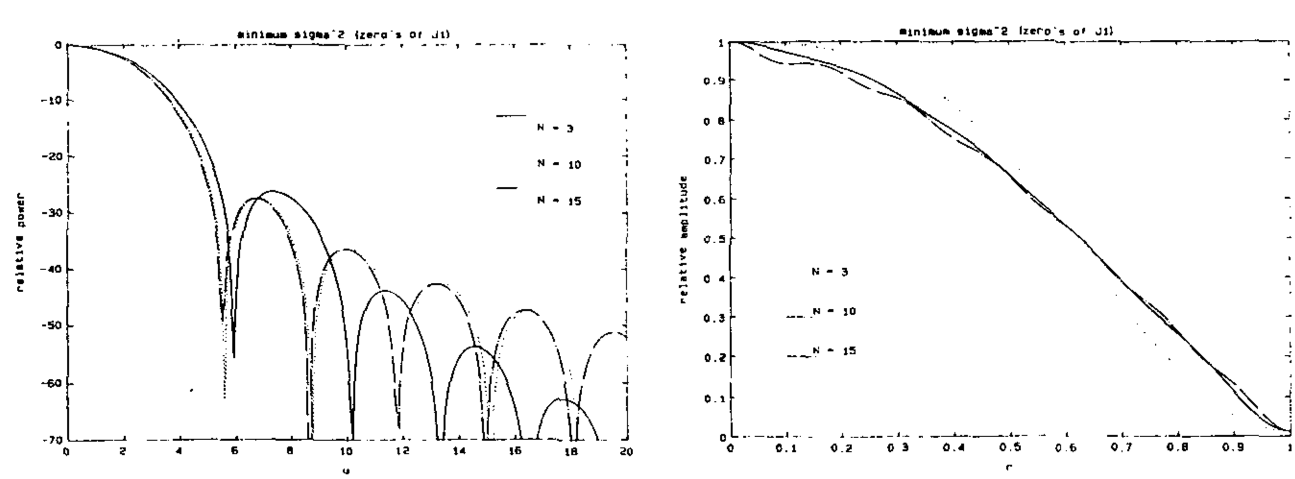

Figure 4.3 g(u) and f(r) for minimum σ^2; using the series $\sum_{n=0}^{N} a_n J_0(\nu_n r)$ with $J_1(\nu_n) = 0$

the illumination is a radial function, which is a solution of the Fredholm integral equation with largest eigenvalue $\alpha(p)$:

$$\alpha(p)S_{00}(p,r) = \int_0^1 S_{00}(p,s)\, J_0(prs)sds \tag{4.15}$$

The functions $S_{00}(p,r)$ are called hyperspheroidal functions. Borgiotti [4] tried to expand these functions in a series of Besselfunctions. In table 1 the coefficients a_n are shown for different values of c, calculated with the method presented in this report.

Table 1 a_n for unconstrained optimization of η_b

c	a_1	a_2	a_3	a_4	a_5	a_6	a_7
½	1	0.021157	−0.008402	0.004790			
1	1	0.084790	−0.032862	0.018650	−0.012402		
2	1	0.338182	−0.118224	0.065765	−0.043411	0.031423	
3	1	0.733818	−0.211754	0.114627	−0.074953	0.054015	
3½	1	0.961843	−0.241602	0.129335	−0.084266	0.060626	−0.046358

Comparing these coefficients with those of Borgiotti shows that there is a difference if c is small (< 1.5). When c is large, only the last few coefficients differ slightly. Fig 4.4 shows the aperture distribution were the difference is largest (c = 1) and the aperture distribution with a small difference (c = 3.5). As can be seen, the difference is mainly localized at the edge. This agrees with the statement of Borgiotti, that the difference between his distribution and the hyperspheroidal function is several percent and is mainly localized at the edge of the aperture ([4],p 655).

The results of the unconstrained optimization of $\eta_a \times \eta_b$, $\frac{\eta_b}{\sigma^2}$ and $\frac{\eta_a \eta_b}{\sigma^2}$ are given in table A3,A4 and A5. Figures 4.5, 4.6 and 4.7 show some typical aperture distributions and far field patterns.

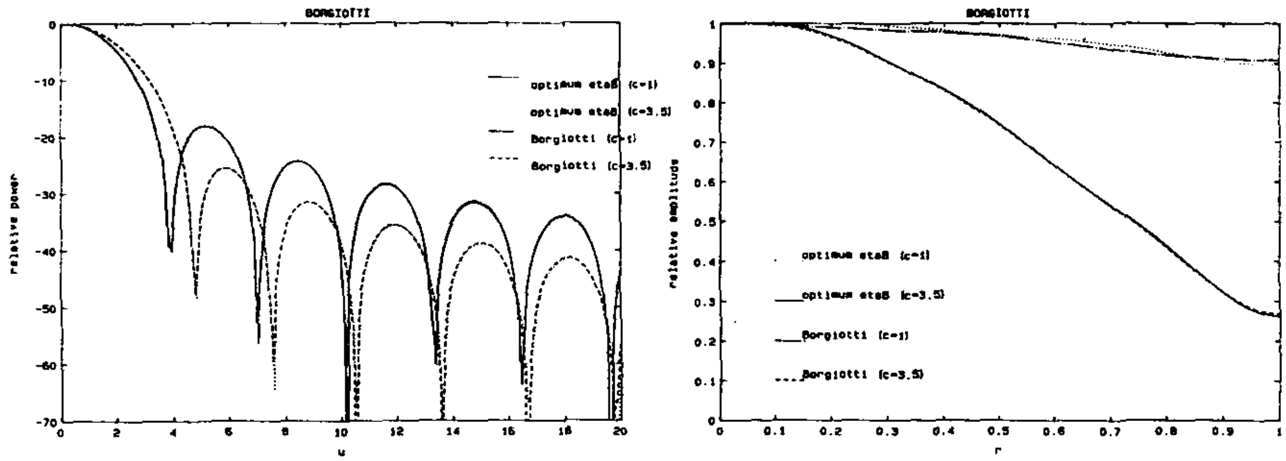

Figure 4.4 g(u) and f(r) for maximum η_b; comparison with the results of Borgiotti

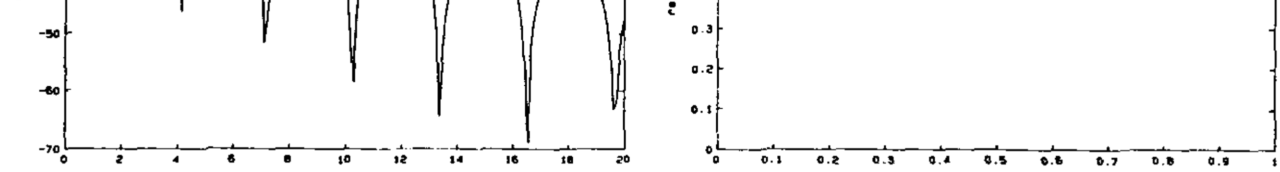

Figure 4.5 g(u) and f(r) for maximum $\eta_a \times \eta_b$; using the series $\sum_{n=0}^{N} a_n J_0(\nu_n r)$ with $J_1(\nu_n) = 0$

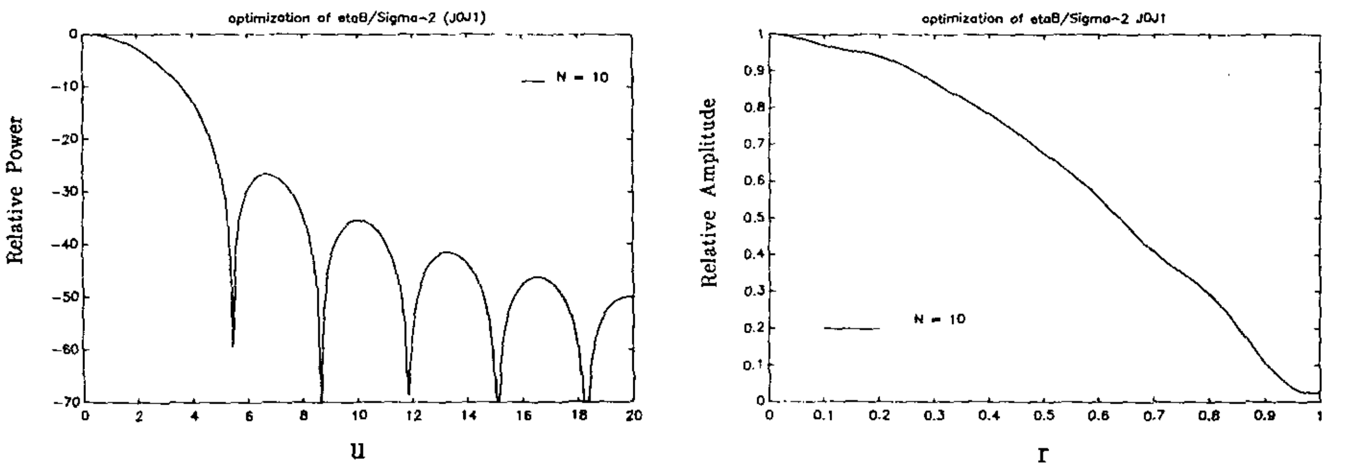

Figure 4.6 g(u) and f(r) for maximum η_b/σ^2; using the series $\sum_{n=0}^{N} a_n J_0(\nu_n r)$ with $J_1(\nu_n) = 0$

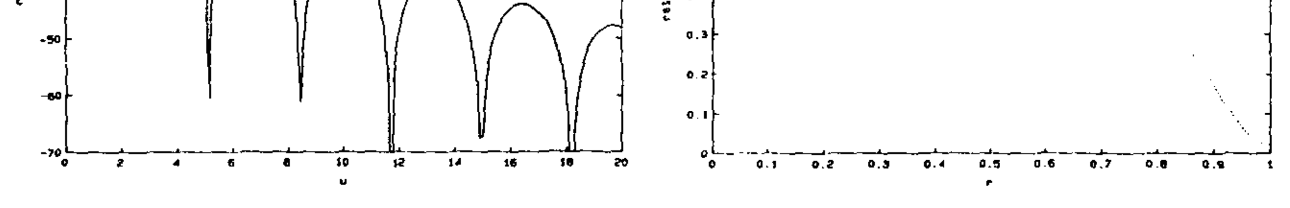

Figure 4.7 g(u) and f(r) for maximum $\eta_a \eta_b/\sigma^2$; using the series $\sum_{n=0}^{N} a_n J_0(\nu_n r)$ with $J_1(\nu_n) = 0$

Table 2 shows the results of the optimum η_a with a number of prescribed side lobes. This can be compared with the results of Taylor (M is the number of equal sidelobe levels, N = 6).

Table 2 constrained optimization of η_a

M	η_a	Taylor	Kriskiy
2	0.9487	0.93	0.945
5	0.8897	0.855	0.890

The computed results are somewhat higher than Taylor's but are in close agreement with those of Kritskiy [17], patterns and aperture distributions similar to one's of Kritskiy are given in figure 4.8.

As an example of constrained optimization a flat topped beam (optimum σ^2) is shown in figure 4.9 and a beam with a specified 3 dB beamwidth (optimum η_b) is given in figure 4.10.

Figure 4.9 shows that if the far field pattern resembles a step the aperture illumination is similar to $J_1(r)/r$.

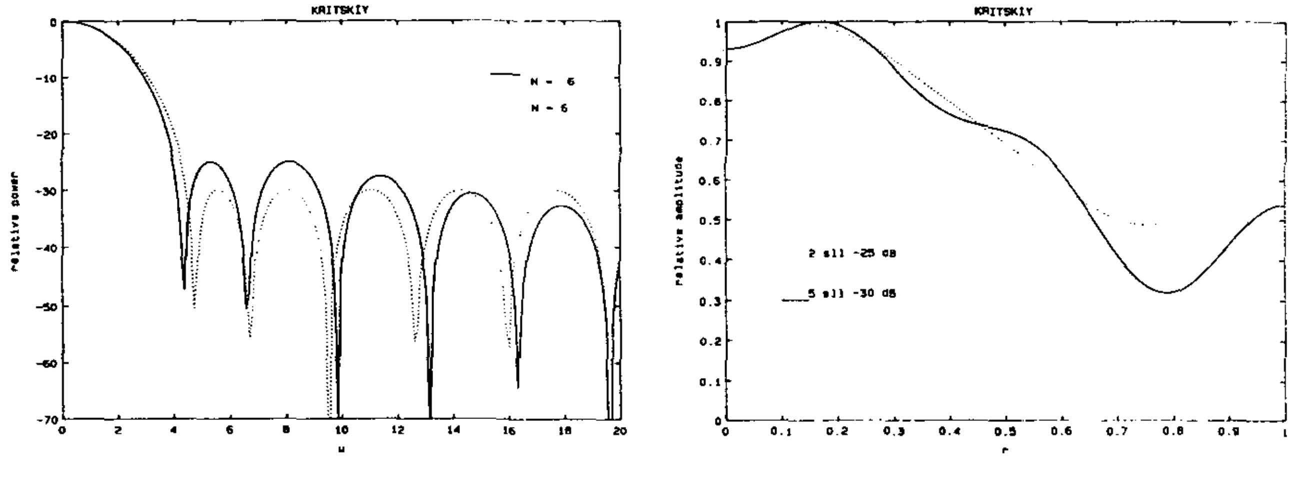

Figure 4.8 g(u) and f(r) for maximum η_a with equal sidelobes; M = 2 and M = 5

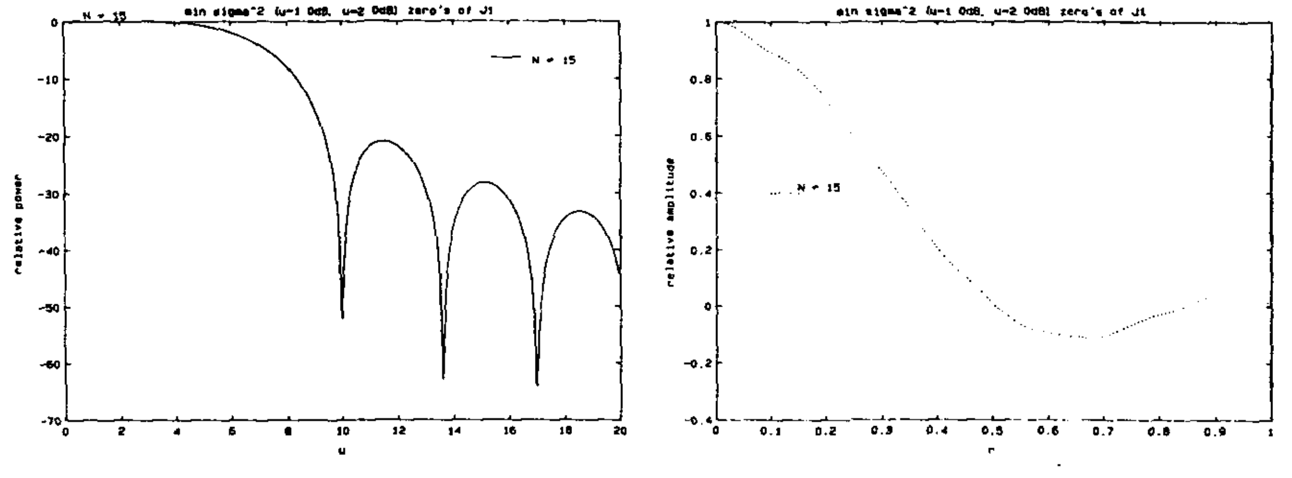

Figure 4.9 g(u) and f(r) for a flat topped beam and minimum σ^2

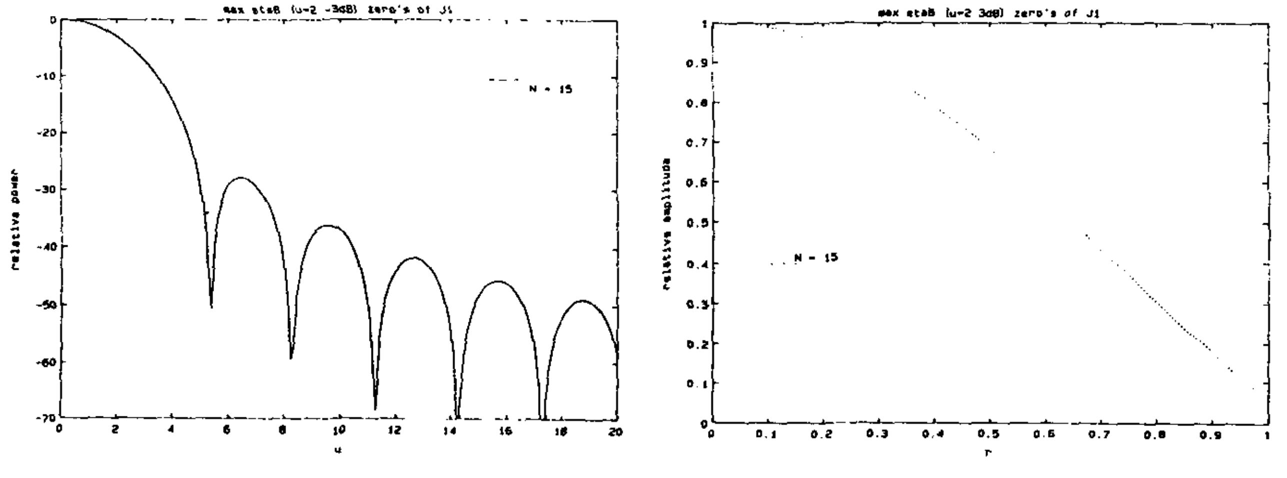

Figure 4.10 g(u) and f(r) for a prescribed 3 dB beamwidth and a maximum η_b

4.1.2 Aperture illumination $\sum_{n=1}^{N} a_n J_0(\nu_n r)$ with $J_0(\nu_n) = 0$

This type of series has been used for synthesis purposes before ([17],[20],[21]). The aperture illumination consists of a series :

$$f(r) = \sum_{n=1}^{N} a_n J_0(\nu_n r) \qquad 0 \leq r \leq 1 \tag{4.16}$$
$$= 0 \qquad \text{elsewhere}$$

with $\nu_1 = 2.4048$, $\nu_2 = 5.5201$,.........(note that n now starts with 1).
Some functions $J_0(\nu_n r)$ are shown in figure 4.10.

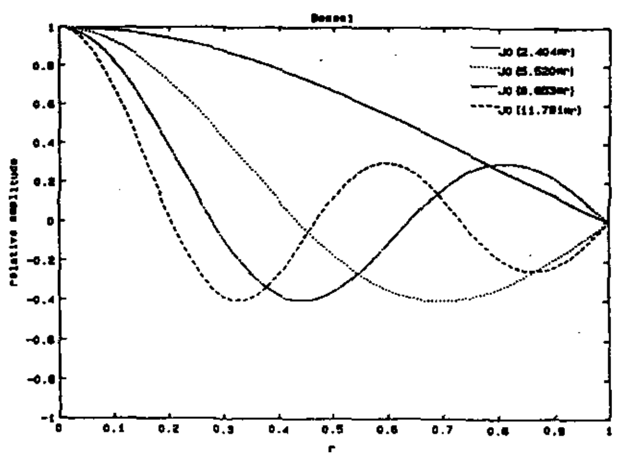

Figure 4.11 $J_0(\nu_n r)$ with $J_0(\nu_n) = 0$.

The far field is (for the case $J_0(\nu_n) = 0$, see (4.3)).

$$g(u) = J_0(u) \sum_{n=1}^{N} \frac{\nu_n a_n}{\nu_n^2 - u^2} J_1(\nu_n) \qquad \text{if } u \neq \nu_n \tag{4.17}$$
$$= \tfrac{1}{2} a_n J_1^2(\nu_n) \qquad \text{if } u = \nu_n$$

This leads to :

$$\underline{e}^T = (J_0(\nu_1 r), \ldots\ldots\ldots J_0(\nu_N r)) \tag{4.18}$$

$$\underline{I}^T(\underline{e}) = J_0(u)\left(\frac{\nu_1 J_1(\nu_1)}{\nu_1^2 - u^2}, \ldots\ldots, \frac{\nu_N J_1(\nu_N)}{\nu_N^2 - u^2}\right). \tag{4.19}$$

Using Lommels equation, [16 p134] gives :

$$A_{ij} = 0 \qquad \text{if } i \neq j \tag{4.20}$$
$$= \tfrac{1}{2} J_1^2(\nu_i) \qquad \text{if } i = j$$

$$X_{ij} = \nu_i \nu_j J_1(\nu_i) J_1(\nu_j) \int_0^c \frac{u\ J_0^2(u)}{(\nu_i^2 - u^2)(\nu_j^2 - u^2)} du \tag{4.21}$$

$$W_{ij} = \nu_i \nu_j J_1(\nu_i) J_1(\nu_j) \int_0^{\pi D/\lambda} \frac{u^3 J_0^2(u)}{(\nu_i^2 - u^2)(\nu_j^2 - u^2)} du \tag{4.22}$$

The elements of the matrices X and W as given in equation (4.21) and (4.22) have to be calculated numerically.

Some examples

The unconstrained optimum for η_a is easy to derive, when making use of equation (3.9). This leads to :

$$\eta_{a,max} = 4(\nu_1^{-2} + \nu_2^{-2} + \ldots\ldots + \nu_N^{-2}) \tag{4.23}$$

$$a^T = \left(\frac{1}{\nu_1 J_1(\nu_1)}, \ldots\ldots\ldots\ldots, \frac{1}{\nu_N J_1(\nu_N)}\right) \tag{4.24}$$

$$g(u) = J_0(u) \sum_{n=1}^{N} \frac{1}{(\nu_n^2 - u^2)} \qquad \text{if } u \neq \nu_n \tag{4.25}$$

$$= \frac{1}{2} \frac{J_1(\nu_n)}{\nu_n} \qquad \text{if } u = \nu_n$$

Table A6 shows the results of the unconstrained optimization of aperture efficiency for some values of N. Some typical aperture distributions and corresponding far field patterns are shown in figure 4.12 (the illumination tends to unity if N becomes large)

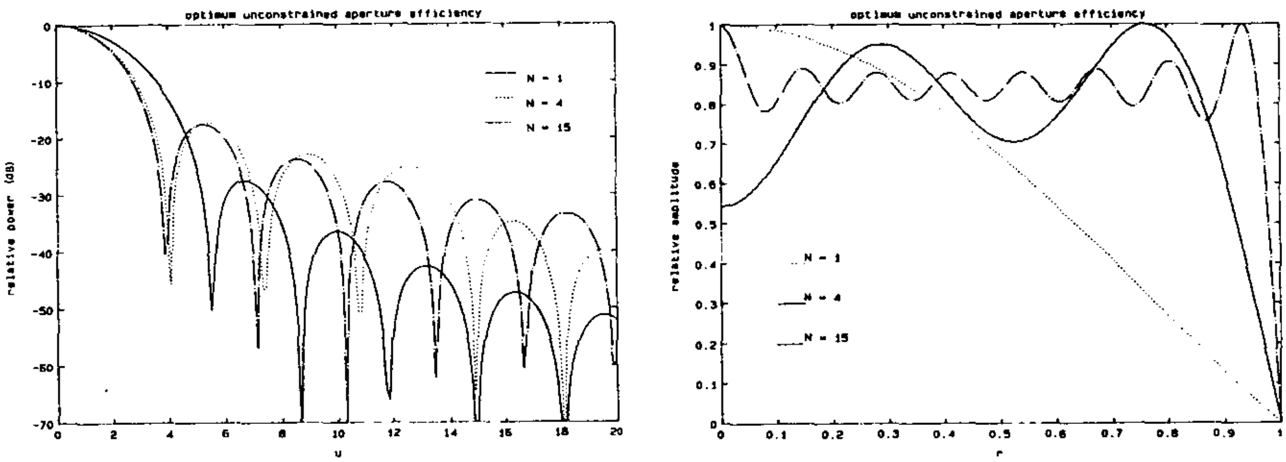

Figure 4.12 g(u) and f(r) for maximum η_a; using the series $\sum_{n=1}^{N} a_n J_0(\nu_n r)$ with $J_0(\nu_n) = 0$

Table A6 shows the results of the unconstrained optimization of σ^2 (figure 4.12 gives an example of g(u) and f(r)). As can be seen the minimum value is close to 5.78. This can be explained by replacing the upper limit of the integral in equation (2.8) by ∞ ([22]). In this case the matrix W becomes diagonal and equation (3.9) can be used leading to $\lambda_{min} = \frac{W_{11}}{A_{11}} = \nu_1^2 = 2.4048^2$. However, this is only allowed if the aperture distribution smoothly approaches zero at the edge. In this report this approximation is not used and the upper limit is kept on $\frac{\pi D}{\lambda}$.

Some of the results of the unconstrained optimization of η_b, $\eta_a \times \eta_b$, and $\frac{\eta_a \eta_b}{\sigma^2}$ are given in tables A7, A8, and A9, respectively. Plots of g(u) and f(r) are shown in figures 4.13 – 4.15.

As an example of constrained optimization a flat topped beam is shown in fig 4.16 and a specified 3 dB beamwidth is shown in fig 4.17. Figure 4.18 shows a pattern with 4 sidelobes of –30 dB.

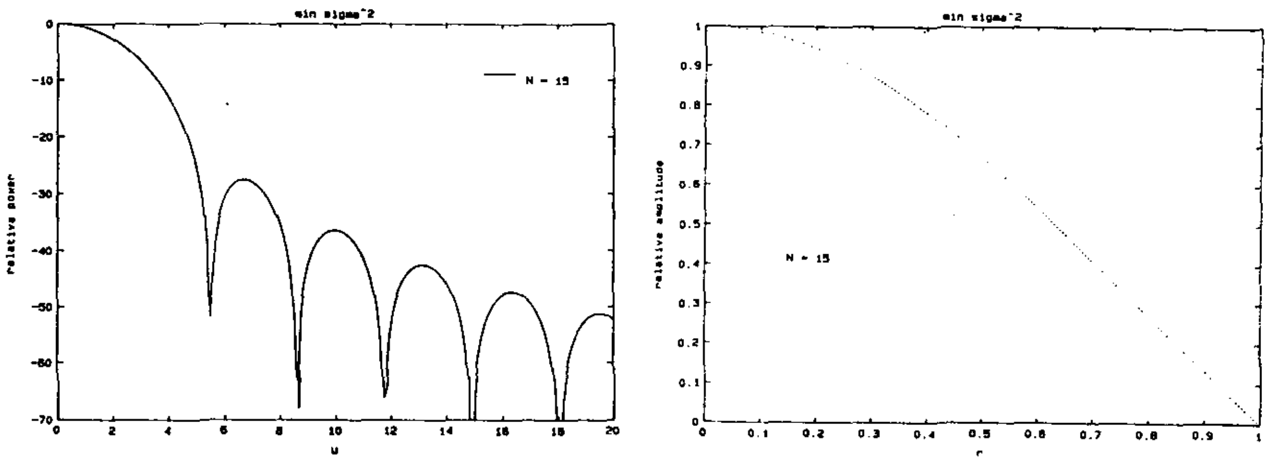

Figure 4.13 g(u) and f(r) for minimum σ^2; using the series $\sum_{n=1}^{N} a_n J_0(\nu_n r)$ with $J_0(\nu_n) = 0$

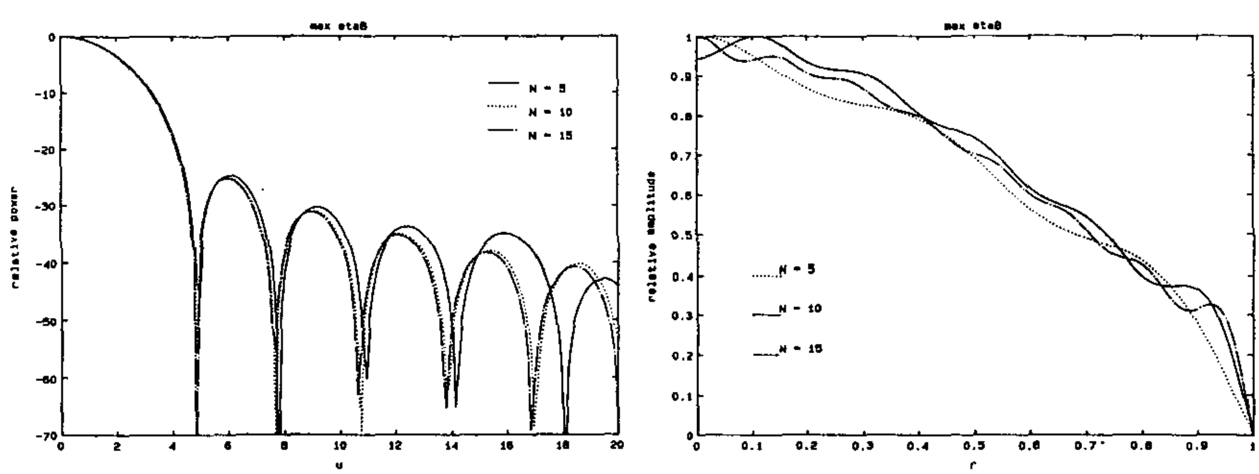

Figure 4.14 g(u) and f(r) for maximum η_b; using the series $\sum_{n=1}^{N} a_n J_0(\nu_n r)$ with $J_0(\nu_n) = 0$

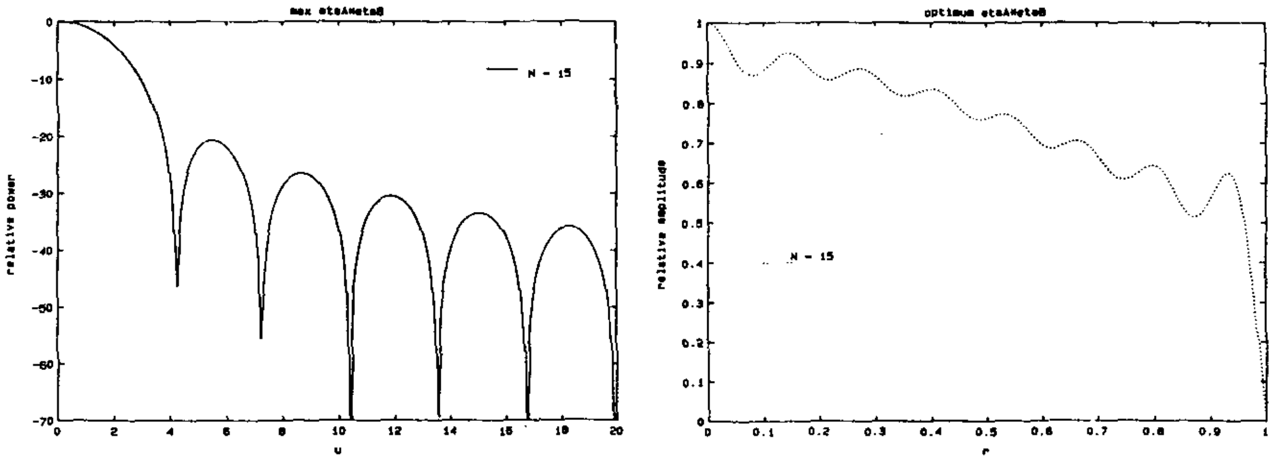

Figure 4.15 g(u) and f(r) for maximum $\eta_a \times \eta_b$; using the series $\sum_{n=1}^{N} a_n J_0(\nu_n r)$ with $J_0(\nu_n) = 0$

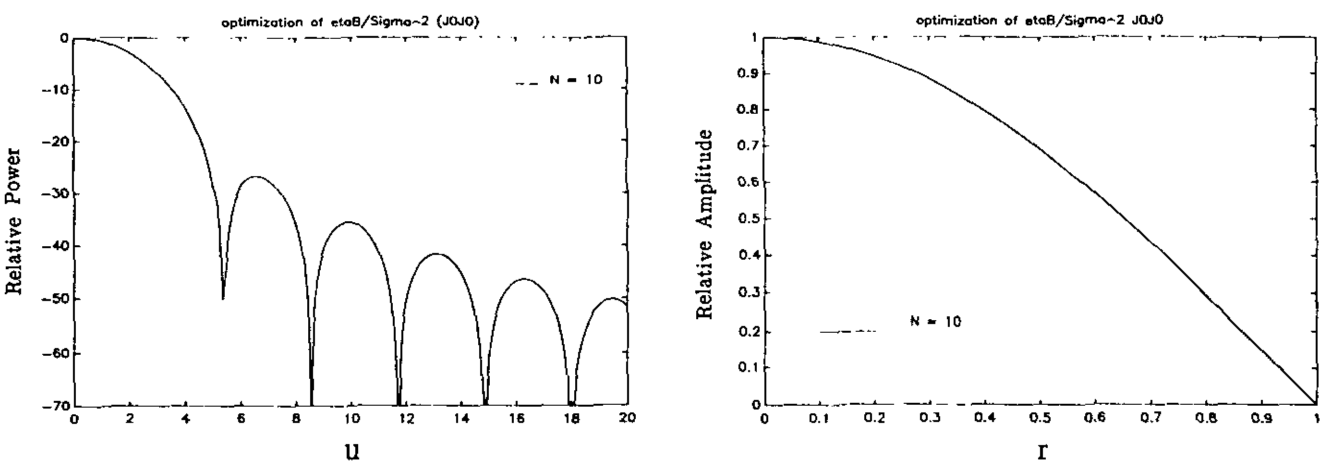

Figure 4.16 g(u) and f(r) for maximum η_b/σ^2; using the series $\sum_{n=1}^{N} a_n J_0(\nu_n r)$ with $J_0(\nu_n) = 0$

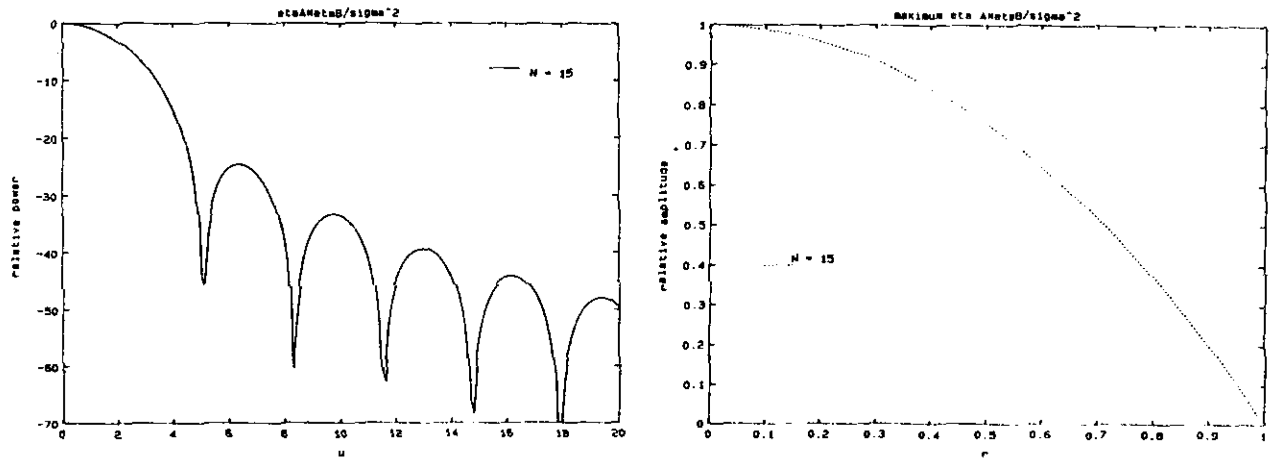

Figure 4.17 g(u) and f(r) for maximum $\eta_a \eta_b / \sigma^2$; using the series $\sum_{n=1}^{N} a_n J_0(\nu_n r)$ with $J_0(\nu_n) = 0$

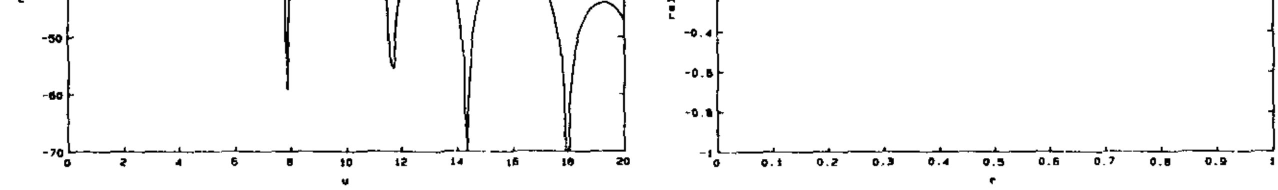

Figure 4.18 g(u) and f(r) for a flat topped beam and minimum σ^2

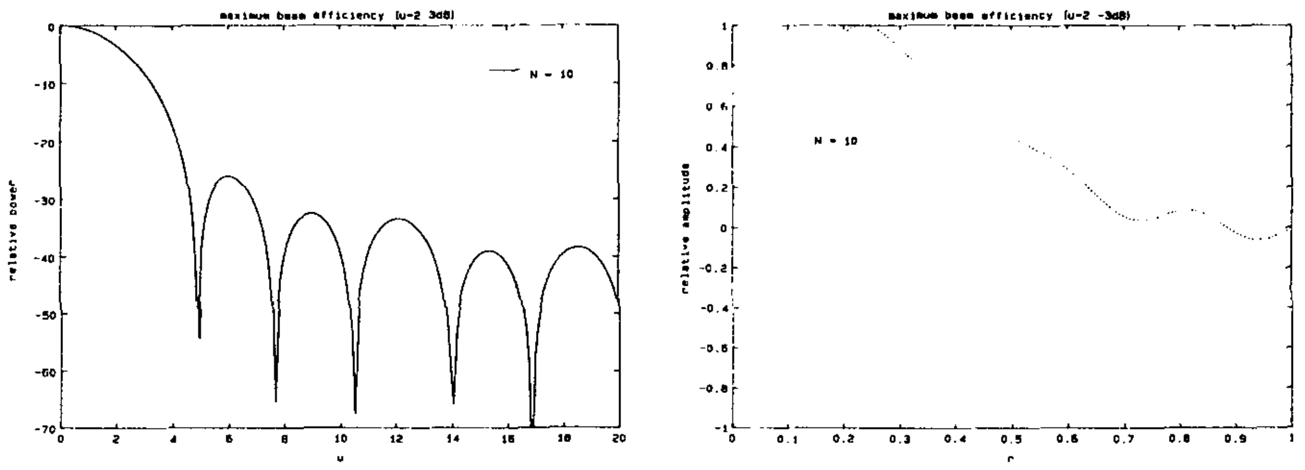

Figure 4.19 g(u) and f(r) for a prescribed 3 dB beamwidth and a maximum η_b

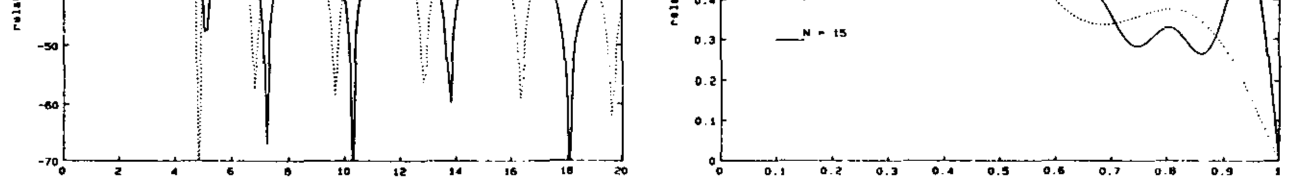

Figure 4.20 g(u) and f(r) with four equal sidelobes and maximum η_a

4.2 Aperture illumination consisting of Zernike polynomials

Other aperture illuminations which can be used for optimization purposes are the circle polynomials of Zernike ([23],[24]) $R^0_{2n}(r)$ (this method is very similar to the method used by Galindo [30]). Such functions reduce to Legendre polynomials :

$$R^0_{2n}(r) = P_n(2r^2-1) \tag{4.26}$$

Some Zernike polynomials are shown in figure 4.19.

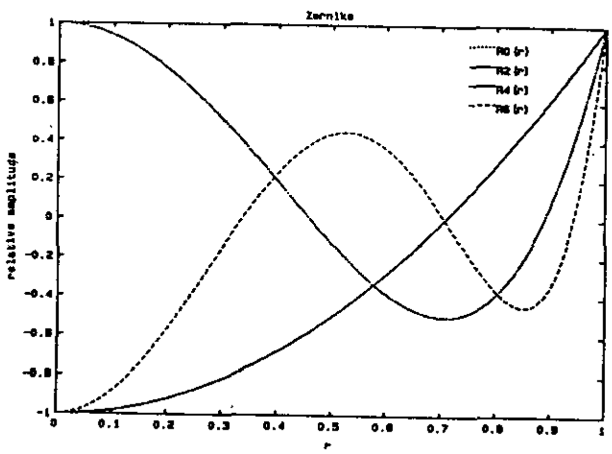

Figure 4.21 Some Zernike polynomials.

g(u) can be calculated by making use of the relation [25] :

$$\int_0^1 R^m_n(r) J_m(ur) r dr = (-1)^{\frac{1}{2}(n-m)} \frac{J_{n+1}(u)}{u} . \tag{4.27}$$

This leads to :

$$g(u) = \sum_{n=0}^{N} a_n \frac{J_{2n+1}(u)}{u} , \tag{4.28}$$

$$\text{so } \underline{e}^T = (R_0^0(r), R_2^0(r), \dots\dots\dots, R_{2N}^0(r)) \tag{4.29}$$

$$I(e) = \left(\frac{J_1(u)}{u}, \frac{J_3(u)}{u}, \dots\dots\dots, \frac{J_{2N+1}(u)}{u} \right). \tag{4.30}$$

The elements of the matrix A can be calculated using [15] :

$$\int_0^1 R_{2i}^0(r) R_{2j}^0(r)\, r\,dr \quad \begin{aligned} &= \frac{1}{4i+2} && \text{if } i = j \\ &= 0 && \text{if } i \neq j. \end{aligned} \tag{4.31}$$

Resulting in :

$$A_{ij} \quad \begin{aligned} &= \frac{1}{4i+2} && \text{if } i = j \\ &= 0 && \text{if } i \neq j \end{aligned} \tag{4.32}$$

The elements of the matrix X can be calculated with the following expression [16,p135] :

$$\int_0^c J_{2i+1}(u) J_{2j+1}(u) \frac{du}{u} = -c \left\{ \frac{J_{2i+2}(c) J_{2j+1}(c) - J_{2i+1}(c) J_{2j+2}(c)}{(2i+1)^2 - (2j+1)^2} \right\} + \quad \text{if } i \neq j$$

$$+ \frac{J_{2i+1}(c) J_{2j+1}(c)}{2i+2j+2} \tag{4.33}$$

and with a modification of Hansens formula [16 p152] :

$$\int_0^c J_{2i+1}^2(u) \frac{du}{u} = \frac{1}{2(2i+1)} \sum_{n=0}^{\infty} \epsilon_n J_{2i+1+n}^2(c) \qquad \text{if } i = j \tag{4.34}$$

where ϵ_n is the Neumanns factor which is defined as :

$\epsilon_n \quad = 1 \qquad$ for $n = 0$

$\qquad = 2 \qquad$ elsewhere.

Calculating the integral as a series of Besselfunctions as in (4.34) is a practical way because most numerical procedures use backward recursive relations, such as

$J_{n-1}(u) = \frac{2n}{u} J_n(u) - J_{n+1}(u)$ to come to $J_{2i+1}(u)$. The reason for this is that an forward way (starting with J_0 and J_1) gives in some cases unstable results. By simply using all the results of $J_{2i+1+n}(c)$, the integral (4.34) can easily be computed.

$$W_{ij} = \int_0^c u\, J_{2i+1}(u) J_{2j+1}(u)\, du \tag{4.35}$$

which has to be calculated numerically.

Some examples

The unconstrained optimum of η_a (using 2.8) leads to :

$$\eta_{a,max} = 1 \tag{4.36}$$

$$a^T = (1, 0, 0, \ldots\ldots 0) \tag{4.37}$$

$$g(u) = \frac{J_1(u)}{u} \tag{4.38}$$

The results of the unconstrained optimization of σ^2, η_b, $\eta_a \times \eta_b$, η_b/σ^2 and $\eta_a \eta_b/\sigma^2$ are given in tables A12, A13, A14, A15 and A16 respectively. Plots of g(u) and f(r) are shown in figures 4.22, 4.23, 4.24, 4.25 and 4.26. The results of the optimization of η_b can be compared with literature [5].
As can be seen in fig 4.24 the results are identical.

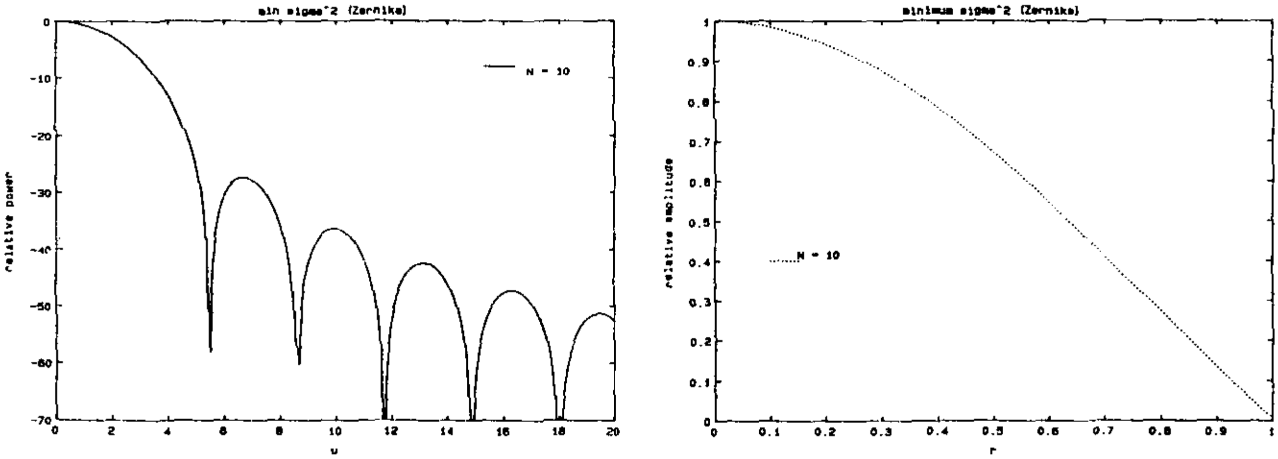

Figure 4.22 g(u) and f(r) for minimum σ^2; using the series $\sum_{n=0}^{N} a_n R_{2n}^0(r)$

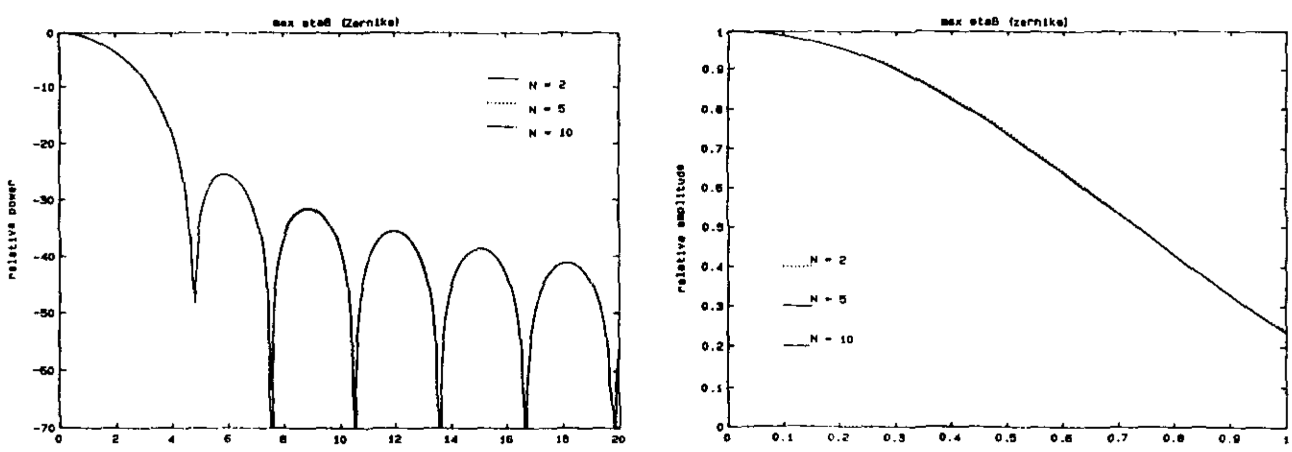

Figure 4.23 g(u) and f(r) for maximum η_b; using the series $\sum_{n=0}^{N} a_n R_{2n}^0(r)$

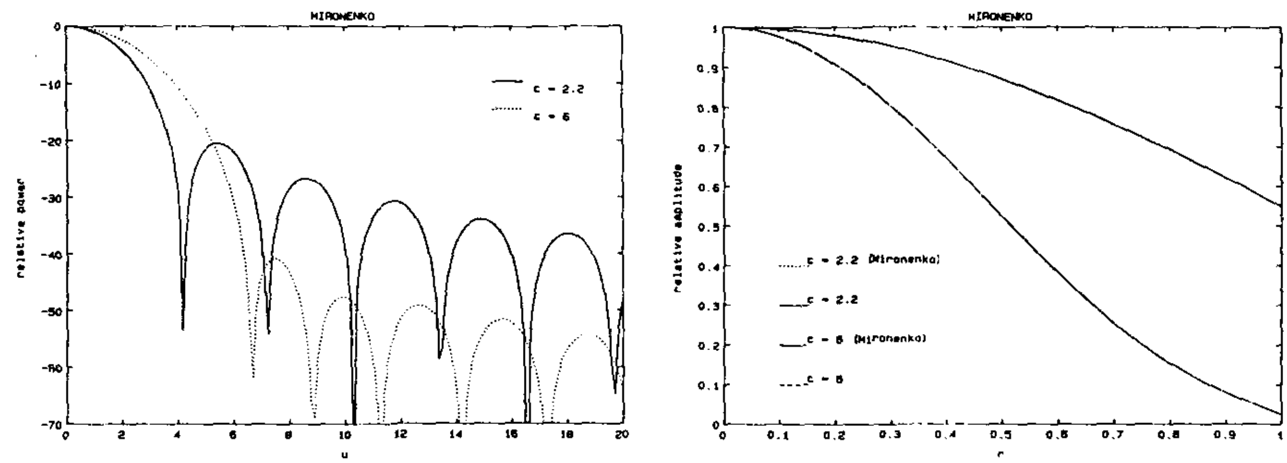

Figure 4.24 g(u) and f(r) for maximum η_b; comparison with the results of Mironenko

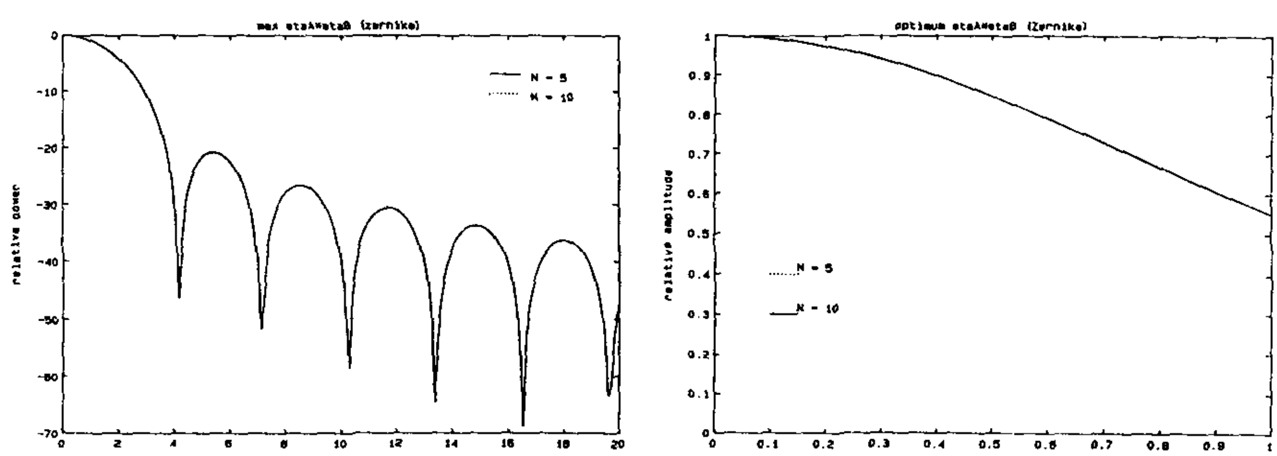

Figure 4.25 g(u) and f(r) for maximum $\eta_a \times \eta_b$; using the series $\sum_{n=0}^{N} a_n R_{2n}^{0}(r)$

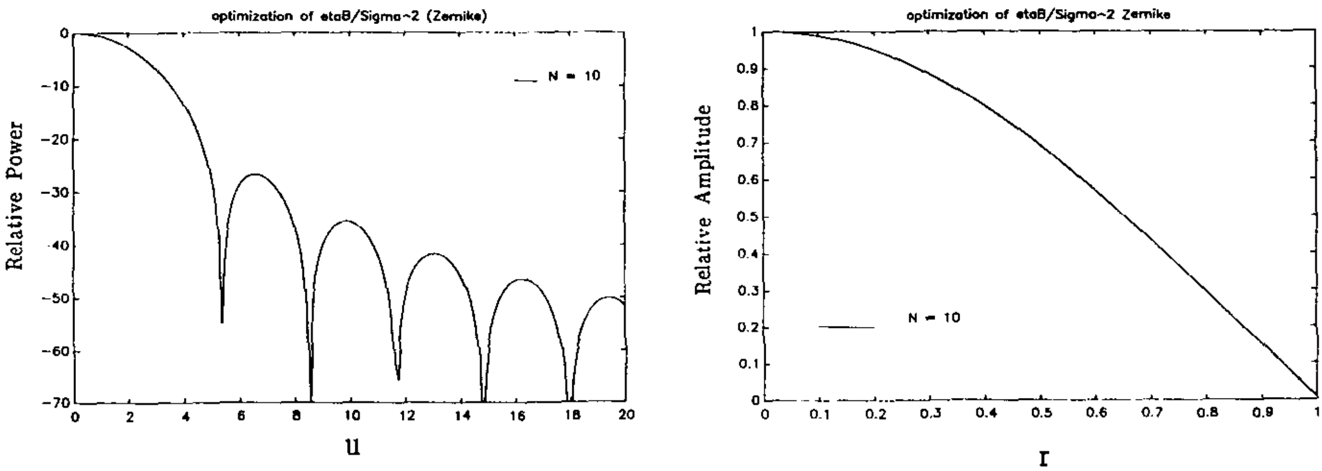

Figure 4.26 g(u) and f(r) for maximum η_b/σ^2; using the series $\sum_{n=0}^{N} a_n R^0_{2n}(r)$

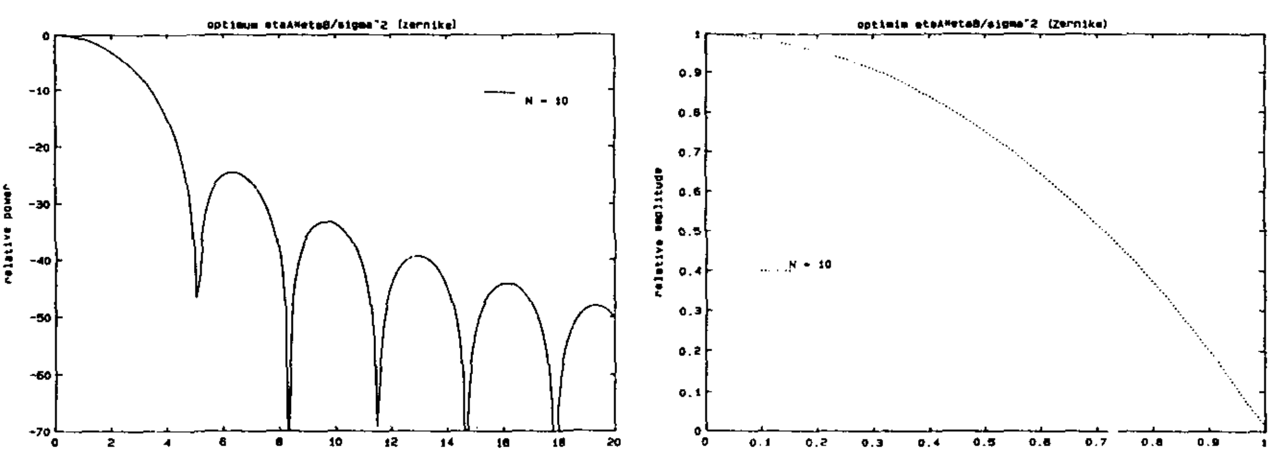

Figure 4.27 g(u) and f(r) for maximum $\eta_a\eta_b/\sigma^2$; using the series $\sum_{n=0}^{N} a_n R^0_{2n}(r)$

4.3 Aperture illumination consisting of power–law functions

Some engineers use an aperture distribution which consists of a series of powers of $(1-r^2)$ (see e.g.[8]) :

$$f(r) = \sum_{n=0}^{N} a_n (1-r^2)^n \tag{4.39}$$

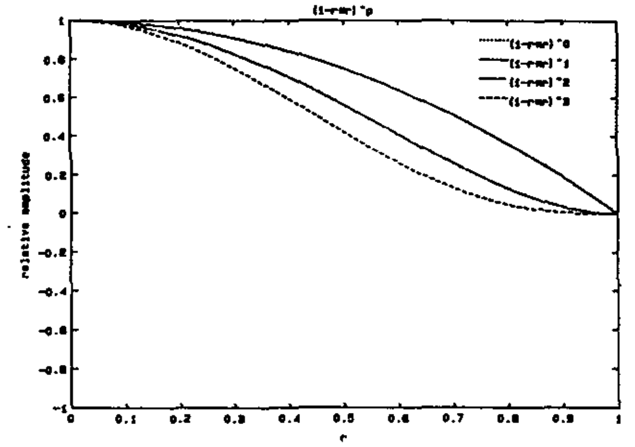

Figure 4.28 Some powers of $(1-r^2)^n$.

The reason for this is that in some practical cases the functions f(r) are smooth monotonically decreasing functions which can be approximated by a few terms of the series stated in (4.39)[26].

g(u) can be calculated with the following relation:

$$\int_0^1 (1-r^2)^n J_0(ur) r dr = 2^n\, n!\, \frac{J_{n+1}}{u^{n+1}} \tag{4.40}$$

Resulting in :

$$g(u) = \sum_{n=0}^{N} a_n 2^n\, n!\, \frac{J_{n+1}}{u^{n+1}} \tag{4.41}$$

So $\underline{e}^T = (1, (1-r^2), \ldots\ldots\ldots, (1-r^2)^N)$ (4.42)

$$\underline{I}^T(\underline{e}) = (\frac{J_1(u)}{u}, \ldots\ldots\ldots\ldots, 2^n\, n! \frac{J_{n+1}}{u^{n+1}}) \qquad (4.43)$$

The elements of the matrix A are easy to calculate :

$$A_{ij} = \frac{1}{2(i+j+1)} \qquad (4.44)$$

The elements of the matrix X can be calculated with :

$$\int_0^c u^{-i-j-1} J_{i+1}(u) J_{j+1}(u) du = -\frac{c^{-i-j}}{2(i+j+1)} \{J_i(c)J_j(c) + J_{i+1}(c)J_{j+1}(c)\} \qquad (4.45)$$

Resulting in :

$$X_{ij} = (2^{i+j}\, i!j!) - 1 \frac{c^{-i-j}}{2(i+j+1)} \{J_i(c)J_j(c) + J_{i+1}(c)J_{j+1}(c)\} \qquad (4.46)$$

Which have to be calculated numerically.
The elements of the matrix W are :

$$W_{ij} = (2^{i+j}\, i!j!) \int_0^c u^{-i-j+1} J_{i+1}(u) J_{j+1}(u) du \qquad (4.47)$$

which have to be calculated numerically, or solved analytically using [16],p.136.

<u>Some examples</u>

Optimization of η_a gives the same results as in equation (4.36 –4.38).The results of the optimization of σ^2 and η_b are given in table A17 and A18 (plots of g(u) and f(r) in figures 4.29 and 4.30).

The results for optimization of $\eta_a \times \eta_b$, η_b/σ^2 and $\eta_a\eta_b/\sigma^2$ are shown in table A19, A20 and A21 (fig.4.31, fig.4.32 and 4.33 show plots of g(u) and f(r)).

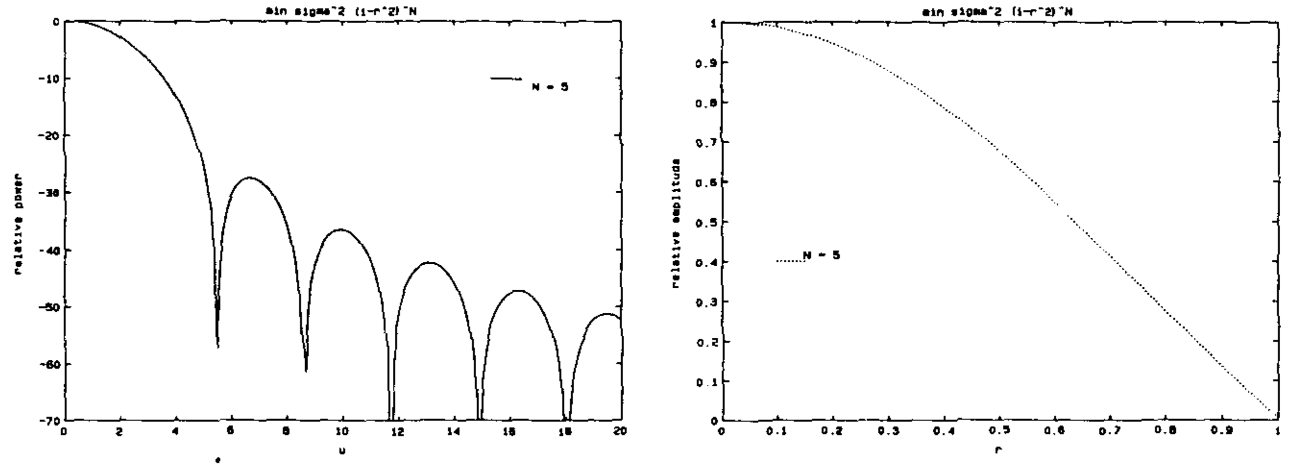

Figure 4.29 g(u) and f(r) for minimum σ^2; using the series $\sum_{n=0}^{N} a_n (1-r^2)^n$

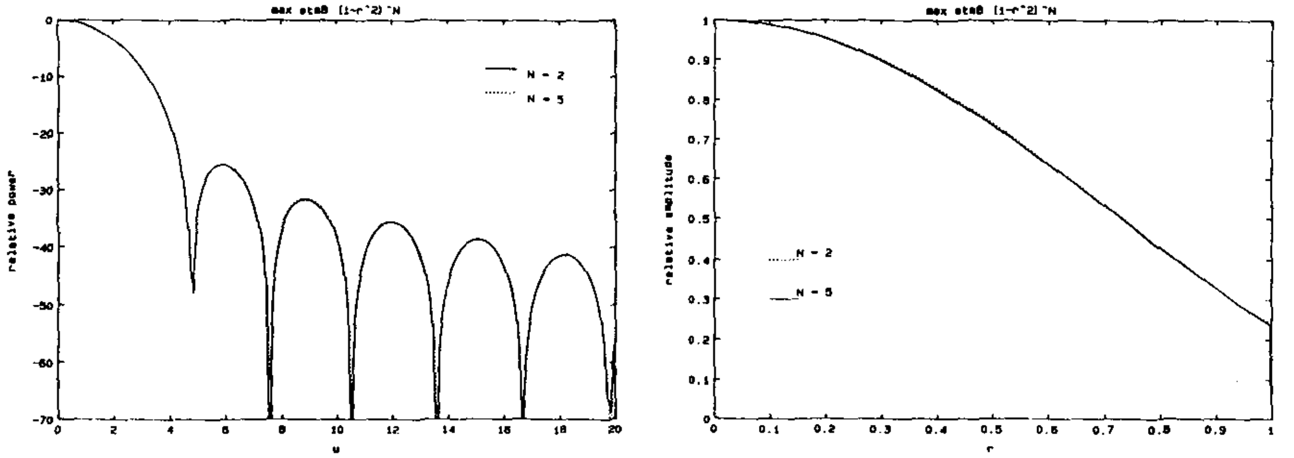

Figure 4.30 g(u) and f(r) for maximum η_b; using the series $\sum_{n=0}^{N} a_n (1-r^2)^n$

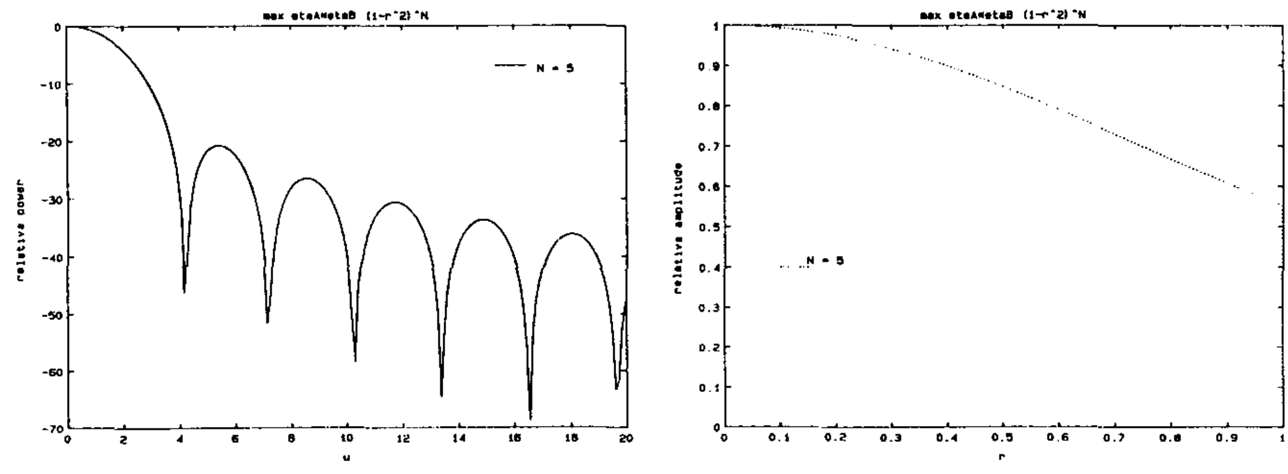

Figure 4.31 g(u) and f(r) for maximum $\eta_a \times \eta_b$; using the series $\sum_{n=0}^{N} a_n (1-r^2)^n$

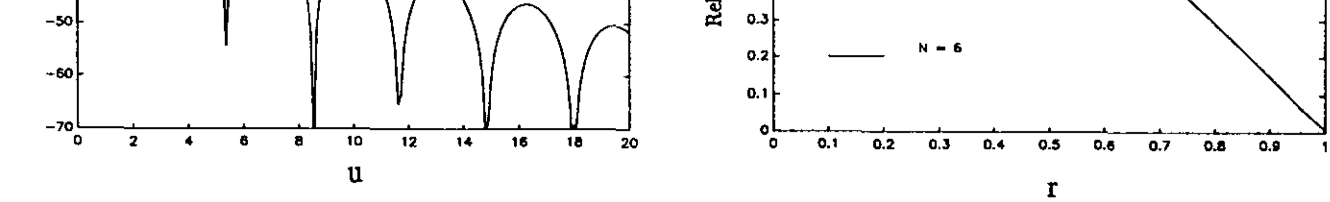

Figure 4.32 g(u) and f(r) for maximum η_b/σ^2; using the series $\sum_{n=0}^{N} a_n (1-r^2)^n$

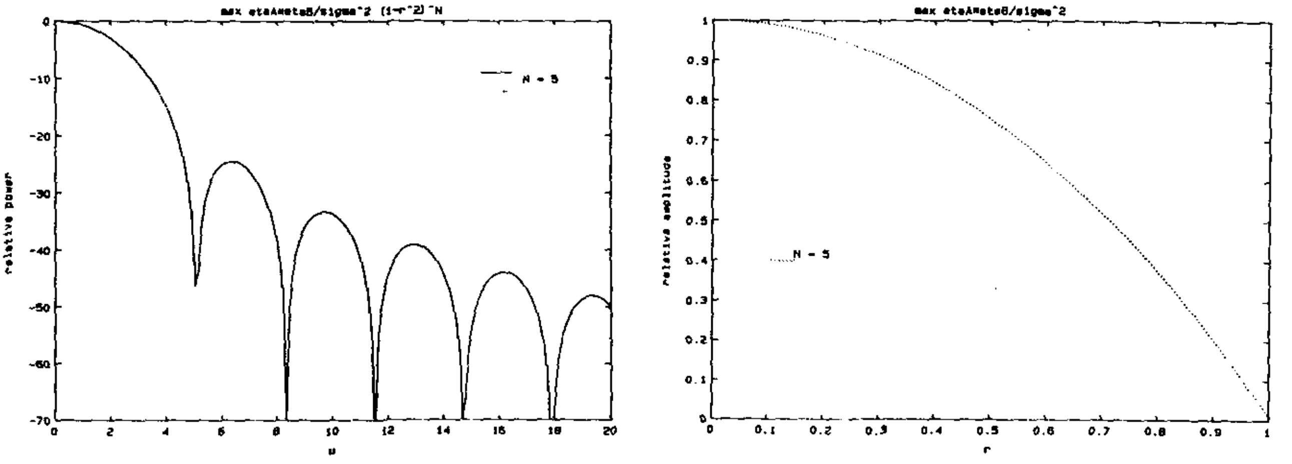

Figure 4.33 g(u) and f(r) for maximum $\eta_a \eta_b / \sigma^2$; using the series $\sum_{n=0}^{N} a_n (1-r^2)^n$

5 Comparing different kinds of source functions

Up to now, different kinds of source functions have been considered. It is interesting to see what kind of function is best suited for particular optimization purposes. If the tables A1 – A21 are scrutinized, it becomes clear that for different optimization purposes, different kinds of source functions should be used.

All the results presented in the tables are summarized in figures 5.1 to 5.6. These figures show the convergence rate of the procedure when the antenna parameters are optimized, using different source functions. The value of the parameters are given against N, where N is the number of elementary functions in the series. From these figures it is easy to deduce the most suitable source function for the optimization of a particular antenna parameter or a product of different antenna parameters.

An optimal η_a is the prime objective with ground–based antennas being part of a communication system. An optimal η_b applies to satellite based antenna systems because it assures a high amount of power in a prescribed region. The optimization of the product $\eta_a\eta_b/\sigma^2$ is interesting for ground based radiometry purposes. As stated before a maximum η_b will ensure a high amount of power in a prescribed region and a minimal σ^2 will assure a small spread around the axis u=0, thus making the sidelobes low. Including the maximization of η_a will prevent the antenna from becoming too large, thereby reducing the costs of the antenna.

Interesting to note is that the optimization of $\eta_a\eta_b/\sigma^2$ resulted in a similar aperture illumination function for all source functions used. This led to the expectation that there was a particular optimum aperture function. Optimization with $(1-r^2)^n$ showed that $(1-r^2)$ was the leading term (a_1 was at least 100 times larger than the other a_n's $(n=0,..N,\neq 1)$). Optimization with Zernike polynomials showed that the first two coefficients a_0 and a_1 were nearly equal and that the other coefficients were at least 500 times smaller. This also led to the conclusion that $(1-r^2)$ is the optimum function because (see 4.26):

$$\left.\begin{array}{l} R_0^0(2r^2-1) = 1 \\ R_2^0(2r^2-1) = 2r^2-1 \end{array}\right\} -0.5R_0^0(2r^2-1)-0.5R_2^0(2r^2-1) = 1-r^2$$

If the upper boundary of the integral in (2.6) is set to ∞, $(1-r^2)$ will be the optimal function. This means that for large antennas (large D/λ), $1-r^2$ optimizes $\eta_a\eta_b/\sigma^2$.

The constrained optimization of the antenna parameters is given in figures 5.6 to 5.14. In these figures the antenna parameter under consideration is optimized, when the sidelobe–level is lower than –25 or –30 dB, respectively. As can be seen from these figures, the Zernike circle polynomials give good results for any optimization which includes η_b. As shown in literature (Slepian [19]) the function which optimizes the beam efficiency is the hyperspheroidal function (because it is the eigenfunction of the Fredholm integral). That Zernike polynomials can approximate this function well, is not surprising because the Zernike polynomials are a limiting case of the hyperspheroidal functions ($p \to 0$ see (4.15)).

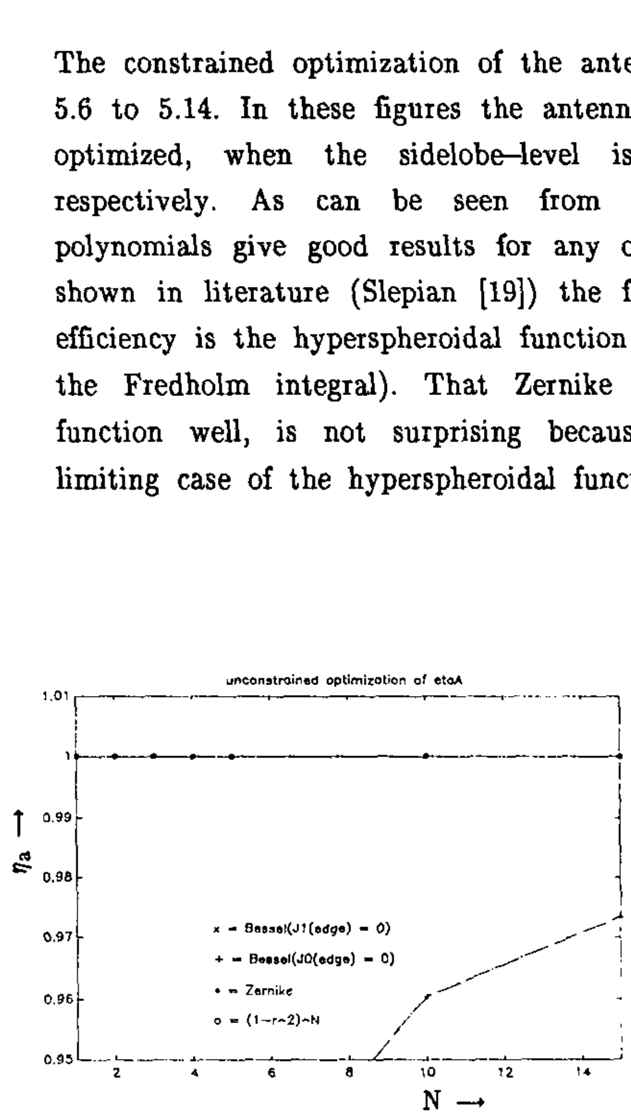

Figure 5.1 The value of η_a against N, where N is the number of elementary functions in the series.

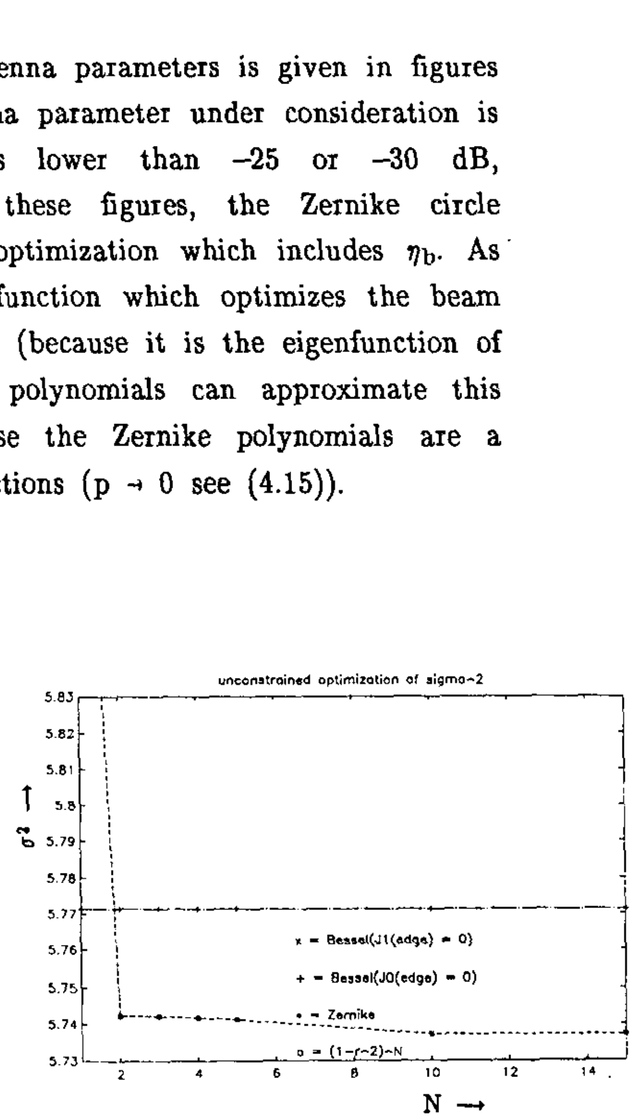

Figure 5.2 The value of σ^2 against N, where N is the number of elementary functions in the series.

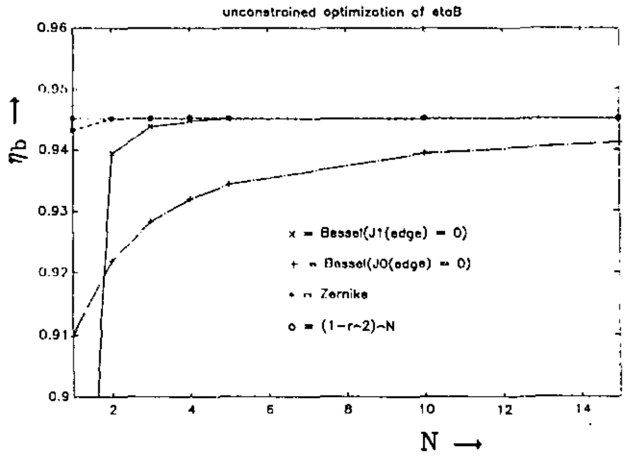

Figure 5.3 The value of η_b against N, where N is the number of elementary functions in the series.

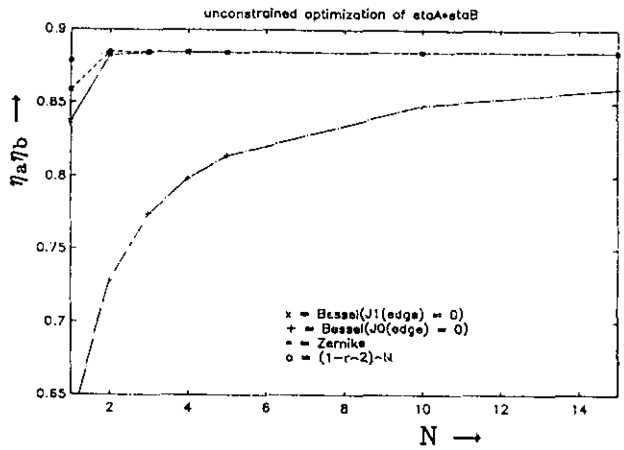

Figure 5.4 The value of $\eta_a\eta_b$ against N, where N is the number of elementary functions in the series.

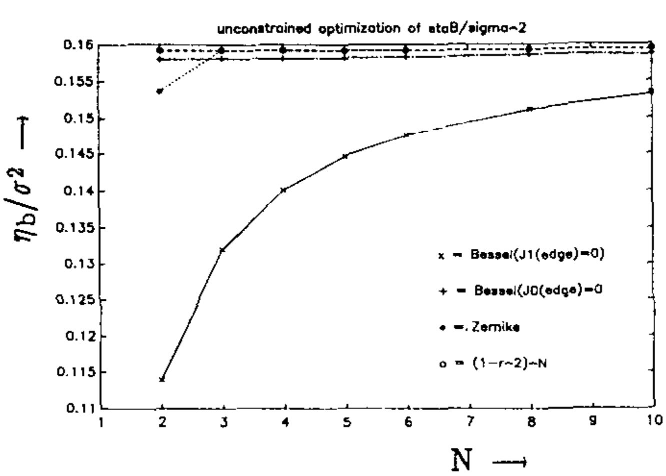

Figure 5.5 The value of η_b/σ^2 against N, where N is the number of elementary functions in the series.

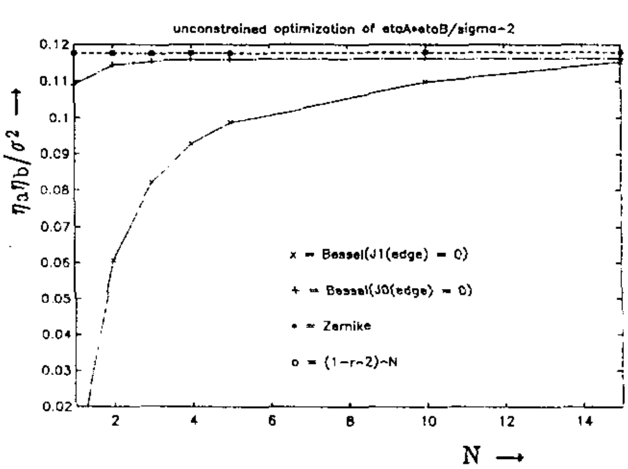

Figure 5.6 The value of $\eta_a\eta_b/\sigma^2$ against N, where N is the number of elementary functions in the series.

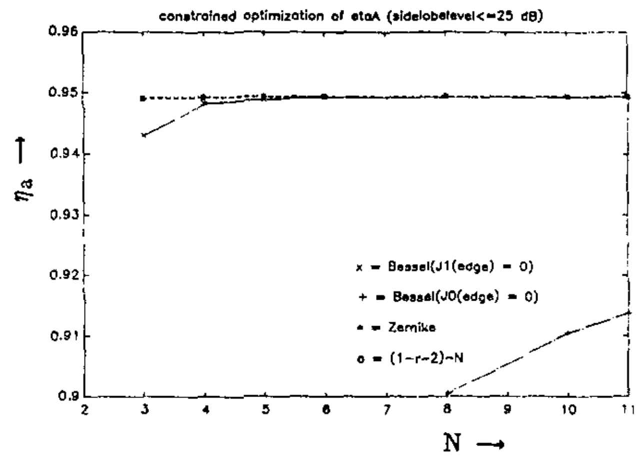

Figure 5.7 The value of η_a against N, while the sidelobes are kept under –25 dB

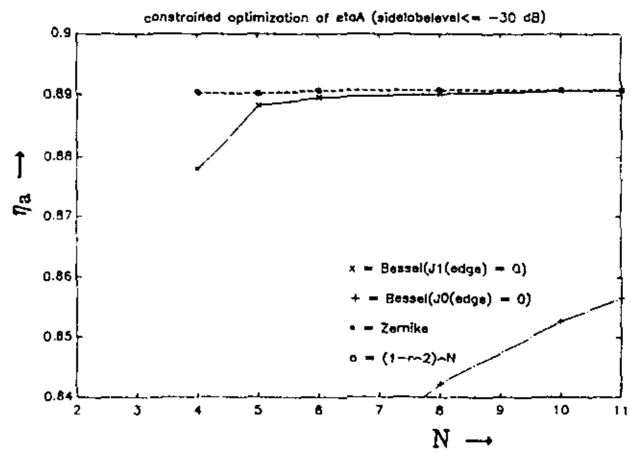

Figure 5.8 The value of η_a against N, while the sidelobes are kept under –30 dB

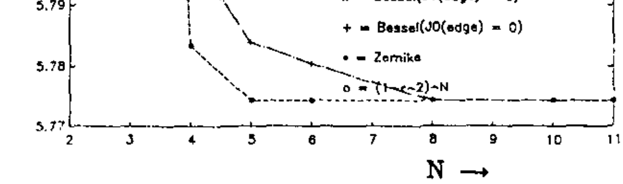

Figure 5.9 The value of σ^2 against N, while the sidelobes are kept under –30 dB

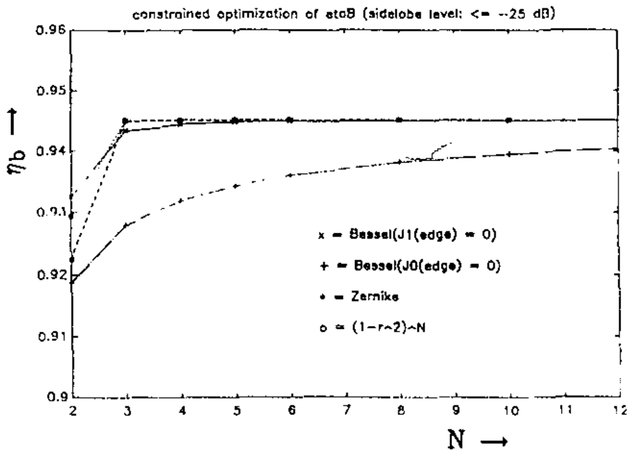

Figure 5.10 The value of η_b against N, while the sidelobes are kept under –25 dB

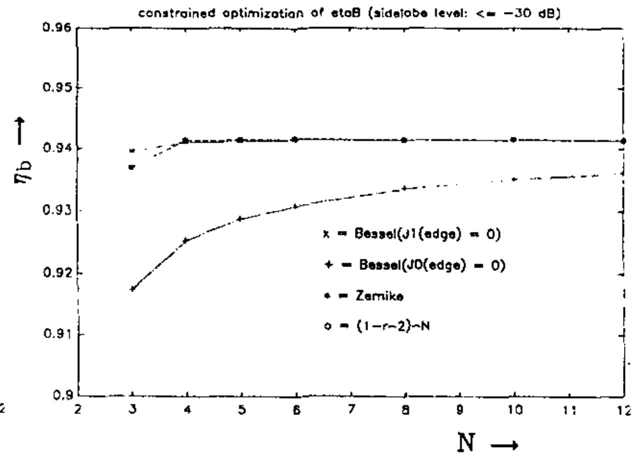

Figure 5.11 The value of η_b against N, while the sidelobes are kept under –30 dB

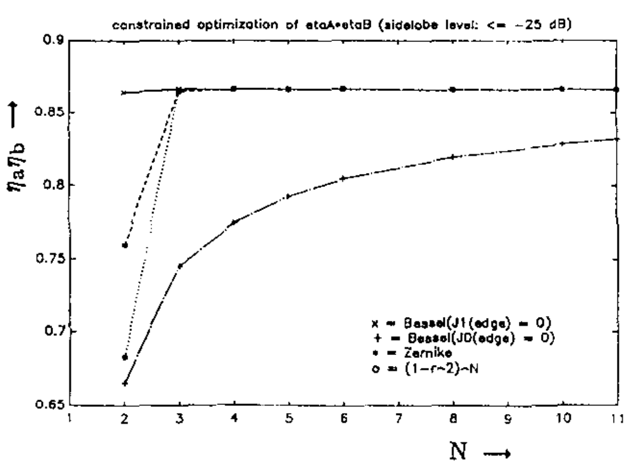

Figure 5.12 The value of $\eta_a\eta_b$ against N, while the sidelobes are kept under –25 dB

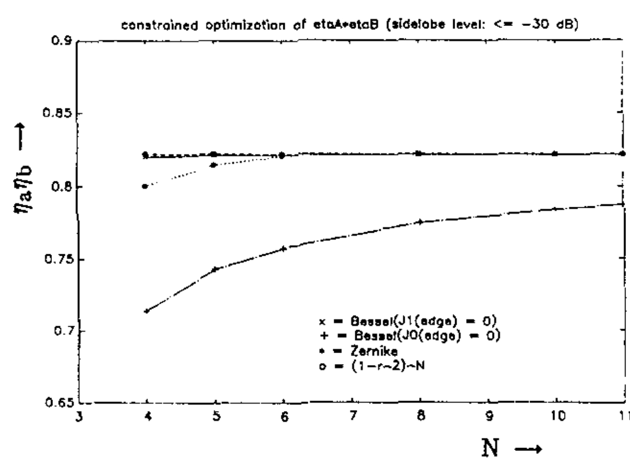

Figure 5.13 The value of $\eta_a\eta_b$ against N, while the sidelobes are kept under –30 dB

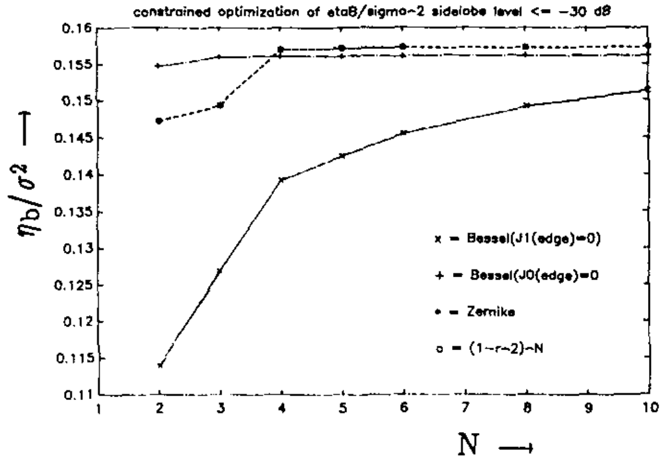

Figure 5.14 The value of η_b/σ^2 against N, while the sidelobes are kept under –30 dB

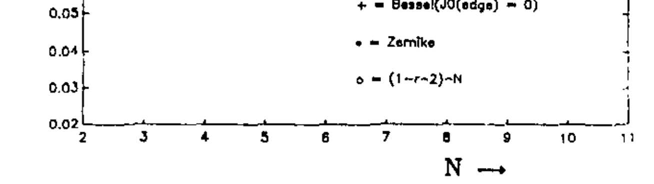

Figure 5.15 The value of $\eta_a\eta_b/\sigma^2$ against N, while the sidelobes are kept under –25 dB

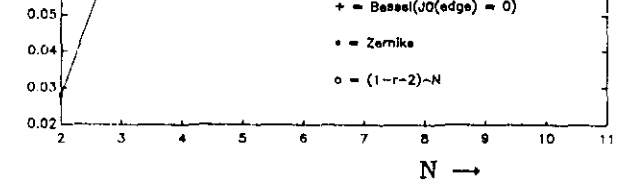

Figure 5.16 The value of $\eta_a\eta_b/\sigma^2$ against N, while the sidelobes are kept under –30 dB

6 Asymmetric patterns

In this section asymmetric patterns are considered. For some purposes asymmetric aperture distributions are preferred to symmetric distributions [27,28]. A suitable aperture distribution is:

$$f(r,\phi) = \sum_{n=1}^{N} a_{n,m} J_m(\nu_{n,m} r) \cos(2m\phi') \tag{6.1}$$

The technique handled now is an extension of the symmetrical case. The theory is similar to that case, but the equations are given for the sake of completeness. Numerical results are not given, but easy to calculate.

g(u) can be calculated with formula (2.1) , substituting (6.1) and using :

$$e^{jur\cos(\phi-m\phi')} = \sum_{p=-\infty}^{\infty} (j)^p J_p(ur) e^{jp(\phi-m\phi')} \tag{6.2}$$

If only even multiples of m are considered (this means that only distributions are considered with two planes of symmetry) this results in :

$$g(u,\phi) = \sum_{n=1}^{N} a_{n,m} \Psi_{n,m} \cos(2m\phi) \tag{6.3}$$

with

$$\Psi_{n,m} = (-1)^m \epsilon_m \int_0^1 J_{2m}(\nu_{n,m} r)\, J_{2m}(ur)\, r\,dr \tag{6.4}$$

and ϵ_m the Neumann factor.

This integral can be calculated with

$$\int_0^1 J_{2m}(\nu_{n,m} r)\, J_{2m}(ur)\, r\,dr = \frac{uJ_{2m}(\nu_{n,m})J_{2m+1}(u) - \nu_{n,m} J_{2m+1}(\nu_{n,m})J_{2m}(u)}{u^2 - \nu^2_{n,m}} \tag{6.5}$$

This can be simplified by choosing $J_{2m}(\nu_{n,m}) = 0$ or $J_{2m+1}(\nu_{n,m}) = 0$ (analogous to

equation 4.4). When $J_{2m}(\nu_{n,m}) = 0$ the distribution is zero at the edge and 6.1 becomes a Fourier–Bessel series. In the case of $J_{2m+1}(\nu_{n,m}) = 0$ the derivative is zero at the edge and 6.1 becomes a Dini–series.
Fitting into the vector and or matrix form gives:

$$\underline{e}^T = (J_{2m}(\nu_{1,2m} r), J_{2m}(\nu_{2,2m} r), \ldots\ldots J_{2m}(\nu_{N,2m} r)) \tag{6.6}$$

$$\underline{a}^T = (a_{1,2m}, a_{2,2m}, \ldots\ldots a_{N,2m}) \tag{6.7}$$

$$g(u,\phi) = \underline{a}^T \underline{\Psi}_{n,m} \tag{6.8}$$

The matrices A, X and W can be calculated analogous to the symmetrical case.

7 Blocked aperture distributions

As will be shown next, the method described in section 2, is also able to deal with a blocked aperture distribution ([29],[17]).The aperture distribution now becomes :

$$f(r) = \sum_{n=1}^{N} a_n [J_0(\nu_n r) + b_n Y_0(\nu_n r)] \qquad \xi \leq r \leq 1 \qquad (7.1)$$

This is a very elegant series, because it offers the chance to describe the behaviour of the distribution at the edge (r = 1) and at an arbitrary point $r = \xi$ (which can be the edge of a sub reflector). Four possibilities arise, the aperture distribution:

1) is zero at $r = \xi$ and at $r = 1$
2) is zero at $r = \xi$ and has a zero derivative at $r = 1$
3) has a zero derivative at $r = \xi$ and is zero at $r = 1$
4) has a zero derivative at $r = \xi$ and at $r = 1$

If possibility 1 is considered the distribution becomes :

$$f(r) = \sum_{n=1}^{N} a_n \left[J_0(\nu_n r) - \frac{J_0(\nu_n \xi)}{Y_0(\nu_n \xi)} Y_0(\nu_n r)\right] \qquad \xi \leq r \leq 1 \qquad (7.2)$$

with Y_0 the Besselfunction of the second kind and zeroth order and ν_n a solution of :

$$J_0(\nu_n) - \frac{J_0(\nu_n \xi)}{Y_0(\nu_n \xi)} Y_0(\nu_n) = 0 \, . \qquad (7.3)$$

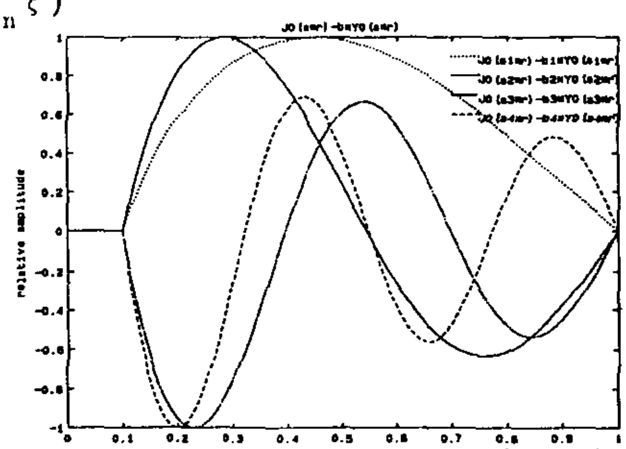

Figure 7.1 Some functions $J_0(\nu_n) - \frac{J_0(\nu_n \xi)}{Y_0(\nu_n \xi)} Y_0(\nu_n)$.

The far field can be calculated using (equation 4.2).

$$g(u) = \sum_{n=1}^{N} a_n \nu_n \frac{\{ J_0(u)\ \alpha_n + J_0(u\xi)\ \beta_n \}}{u^2 - \nu_n^2} \qquad \text{if } u \neq \nu_n \qquad (7.4)$$

$$= \frac{a_i}{2} \{ J_1(u_i)\, \alpha_i + J_1(u_i\xi)\, \beta_i \} + \sum_{\substack{n=1 \\ n \neq i}}^{N} a_n \nu_n \frac{\{ J_0(\nu_i)\, \alpha_n + J_0(\nu_i \xi)\, \beta_n \}}{u_i^2 - \nu_n^2} \qquad \text{if } u = \nu_i$$

$$\text{with } \alpha_n = -J_1(\nu_n) + \frac{J_0(\nu_n \xi)}{Y_0(\nu_n \xi)} Y_1(\nu_n)$$

$$\beta_n = \xi \{ J_1(\nu_n \xi) - \frac{J_0(\nu_n \xi)}{Y_0(\nu_n \xi)} Y_1(\nu_n \xi) \}$$

Fitting into the desired form gives :

$$\underline{e}^T = \left(J_0(\nu_1 r) - \frac{J_0(\nu_1 \xi)}{Y_0(\nu_1 \xi)} Y_0(\nu_1 r), \ldots\ldots, J_0(\nu_N r) - \frac{J_0(\nu_N \xi)}{Y_0(\nu_N \xi)} Y_0(\nu_N r) \right) \qquad (7.5)$$

$$\underline{I}^T(\underline{e}) =$$

$$\left(\nu_1 \frac{\{ J_0(u)\, \alpha_1 + J_0(u\xi)\, \beta_1 \}}{u^2 - \nu_1^2}, \ldots, \nu_N \frac{\{ J_0(u)\, \alpha_N + J_0(u\xi)\, \beta_N \}}{u^2 - \nu_N^2} \right) \qquad (7.6)$$

The elements of the matrix A are :

$$A_{ij} = \begin{cases} 0 & \text{if } i \neq j \\ \frac{1}{2} (\alpha_i^2 - \beta_i^2) & \text{if } i = j \end{cases} \qquad (7.7)$$

The elements of the matrix X and W are :

$$X_{ij} = \tag{7.8}$$

$$\int_0^c \frac{\nu_i \nu_j u}{(u^2-\nu_i^2)(u^2-\nu_j^2)} \{\alpha_i\alpha_j J_0^2(u) + (\alpha_i\beta_j + \alpha_j\beta_i)J_0(u)J_0(u\xi) + \beta_i\beta_j J_0^2(u\xi)\}du$$

$$W_{ij} = \tag{7.9}$$

$$\int_0^{\pi D/\lambda} \frac{\nu_i \nu_j u^3}{(u^2-\nu_i^2)(u^2-\nu_j^2)} \{\alpha_i\alpha_j J_0^2(u) + (\alpha_i\beta_j + \alpha_j\beta_i)J_0(u)J_0(u\xi) + \beta_i\beta_j J_0^2(u\xi)\}du$$

which have to be calculated numerically.

Calculations, with this kind of aperture distribution, are done for two values of ξ (0.1 and 0.05). The value of $\xi = 0.1$ can be considered as the blocking of a sub reflector in a large antenna system or the blocking of a feed in a small antenna system. The value of $\xi = 0.05$ can be the blocking of a feed in a intermediate antenna system. The numerical results are given in tables A18–A22 for $\xi = 0.1$ and in table A23–A27 for $\xi = 0.05$. Corresponding plots for $\xi = 0.1$ are shown in figures 7.2 – 7.6.

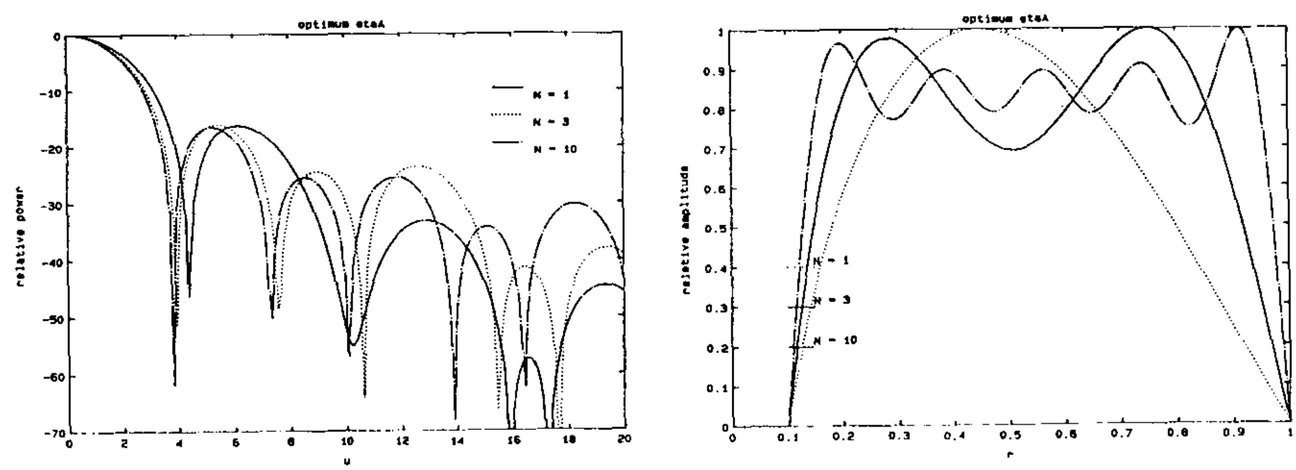

Figure 7.2 g(u) and f(r) for maximum η_a (blocked, aperture zero at $\xi = 0.1$)

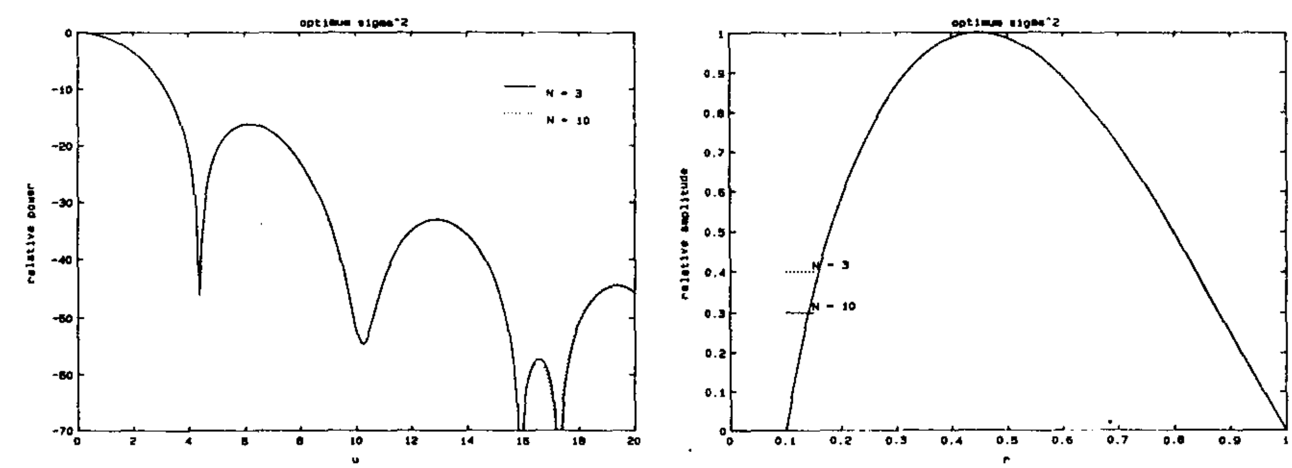

Figure 7.3 g(u) and f(r) for minimum σ^2 (blocked, aperture zero at $\xi = 0.1$)

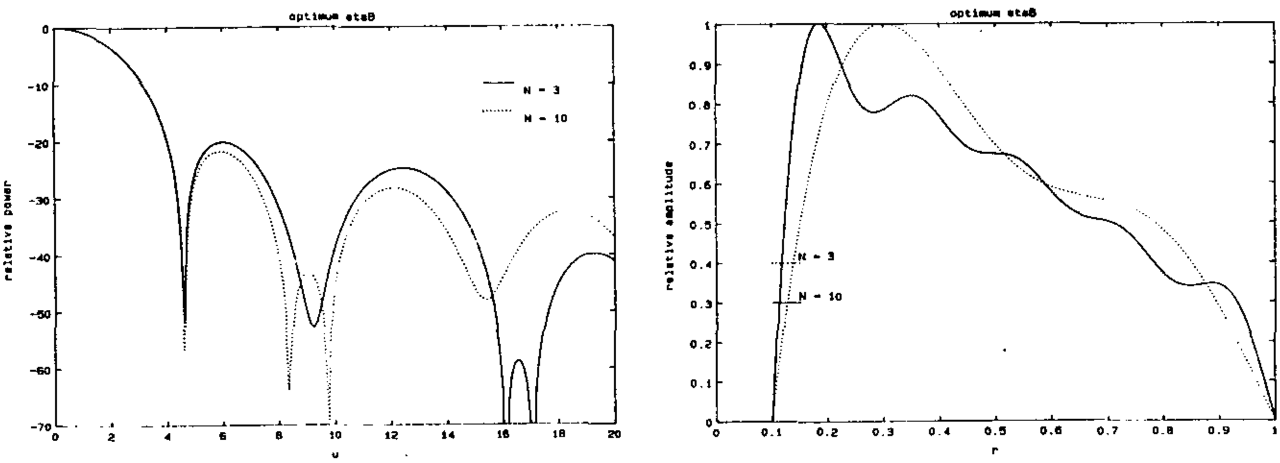

Figure 7.4 g(u) and f(r) for maximum η_b (blocked, aperture zero at $\xi = 0.1$)

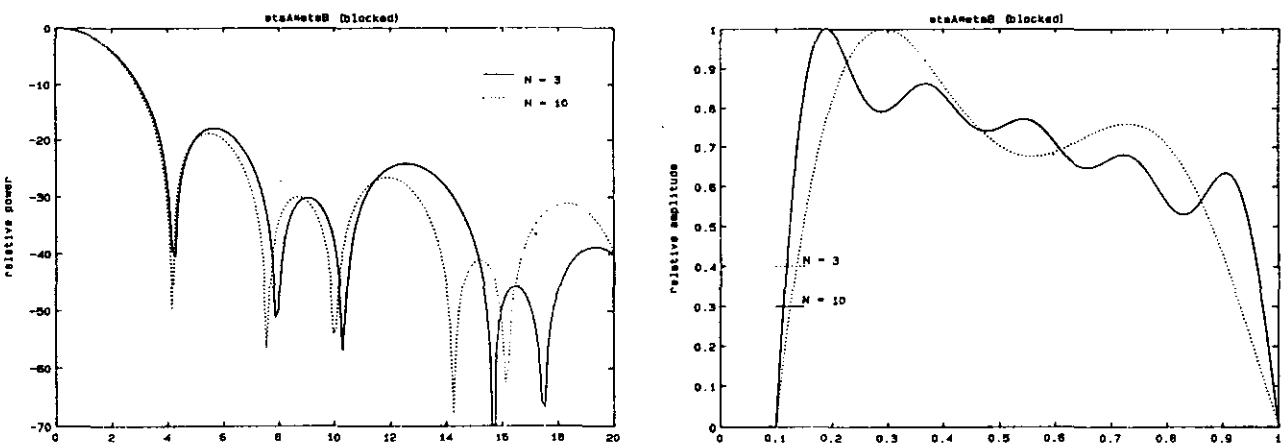

Figure 7.5 g(u) and f(r) for max. $\eta_a \times \eta_b$ (blocked, aperture zero at $\xi = 0.1$)

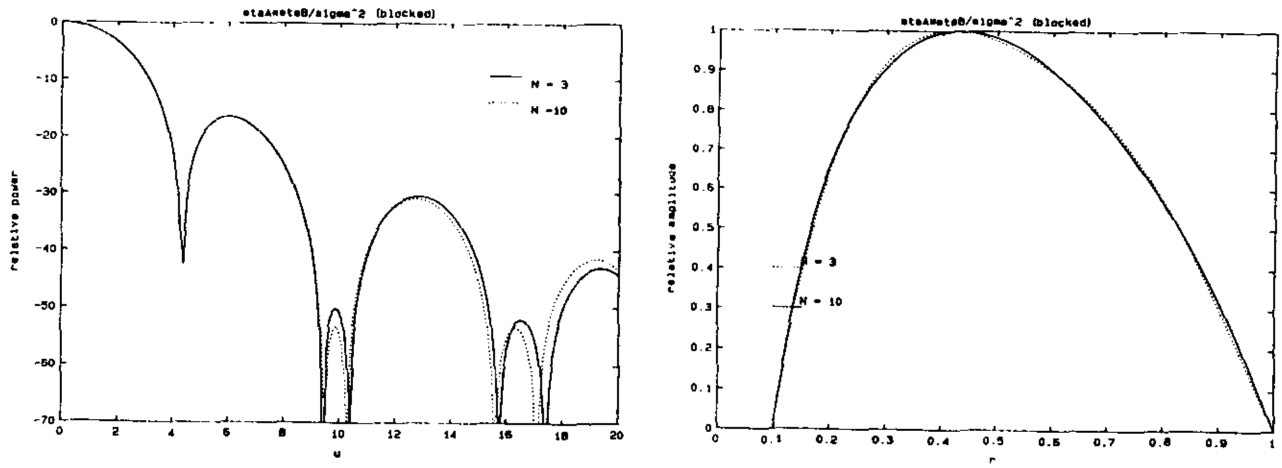

Figure 7.6 g(u) and f(r) for max. $\eta_a \eta_b / \sigma^2$ (blocked, aperture zero at ξ =0.1)

Next possibility 3 is considered, the distribution then becomes :

$$f(r) = \sum_{n=1}^{N} a_n \left[J_0(\nu_n r) - \frac{J_1(\nu_n \xi)}{Y_1(\nu_n \xi)} Y_0(\nu_n r) \right] \qquad \xi \leq r \leq 1 \qquad (7.10)$$

with Y_0 (Y_1) the Besselfunction of the second kind and zeroth (first) order and ν_n a solution of :

$$J_0(\nu_n) - \frac{J_1(\nu_n \xi)}{Y_1(\nu_n \xi)} Y_0(\nu_n) = 0 \qquad (7.11)$$

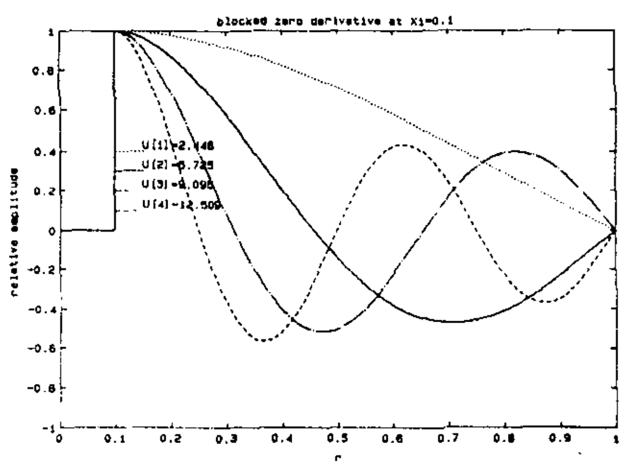

figure 7.7 Some functions $J_0(\nu_n r) - \frac{J_1(\nu_n \xi)}{Y_1(\nu_n \xi)} Y_0(\nu_n r)$.

The far field can be calculated using (equation 4.2).

$$g(u) = \sum_{n=1}^{N} a_n \frac{\{\nu_n J_0(u)\, \alpha_n + uJ_1(\xi u)\, \gamma_n\}}{u^2 - \nu_n^2} \qquad \text{if } u \neq \nu_n \tag{7.12}$$

$$= -\frac{a_i}{2}\{J_1(\nu_i)\, \alpha_i + \xi J_0(\nu_i \xi)\, \gamma_i\} + \sum_{\substack{n=1 \\ n \neq i}}^{N} a_n \frac{\{\nu_n J_0(\nu_i)\, \alpha_n + uJ_1(\nu_i \xi)\, \gamma_n\}}{u_i^2 - \nu_n^2} \qquad \text{if } u = \nu_i$$

$$\text{with } \alpha_n = -J_1(\nu_n) + \frac{J_1(\nu_n \xi)}{Y_1(\nu_n \xi)} Y_1(\nu_n) \tag{7.13}$$

$$\gamma_n = \xi\, \{-J_0(\nu_n \xi) + \frac{J_1(\nu_n \xi)}{Y_1(\nu_n \xi)} Y_0(\nu_n \xi)\}$$

Fitting this into the desired form gives :

$$\underline{e}^T =$$

$$(J_0(\nu_1 r) - \frac{J_1(\nu_1 \xi)}{Y_1(\nu_1 \xi)} Y_0(\nu_1 r), .., J_0(\nu_N r) - \frac{J_1(\nu_N \xi)}{Y_1(\nu_N \xi)} Y_0(\nu_N r)) \tag{7.14}$$

$$\underline{I}^T(\underline{e}) =$$

$$\left(\frac{\{\nu_1 J_0(u)\, \alpha_1 + uJ_1(\xi u)\, \gamma_1\}}{u^2 - \nu_1^2}, \ldots\ldots, \frac{\{\nu_N J_0(u)\, \alpha_N + uJ_1(\xi u)\, \gamma_N\}}{u^2 - \nu_N^2}\right) \tag{7.15}$$

The elements of the matrix A are :

$$A_{ij} = \begin{cases} 0 & \text{if } i \neq j \\ \frac{1}{2}(\alpha_i^2 - \gamma_i^2) & \text{if } i = j \end{cases} \tag{7.16}$$

The elements of the matrix X and W are :

$$X_{ij} = \int_0^c \frac{u}{(u^2-\nu_i^2)(u^2-\nu_j^2)} \{ a_i a_j \nu_i \nu_j J_0^2(u) + (a_i \nu_i \gamma_j + a_j \nu_j \gamma_i) u J_0(u) J_1(u\xi) + u^2 \gamma_i \gamma_j J_1^2(u\xi) \} \, du \tag{7.17}$$

$$W_{ij} = \int_0^{\pi D/\lambda} \frac{u^3}{(u^2-\nu_i^2)(u^2-\nu_j^2)} \{ a_i a_j \nu_i \nu_j J_0^2(u) + (a_i \nu_i \gamma_j + a_j \nu_j \gamma_i) u J_0(u) J_1(u\xi) + u^2 \gamma_i \gamma_j J_1^2(u\xi) \} \, du \tag{7.18}$$

which have to be calculated numerically.

Again calculations are performed with $\xi = 0.1$ and $\xi = 0.05$. Results are shown in tables A28–A32 ($\xi = 0.1$) and A33–A37 ($\xi = 0.05$). Plots are shown in figures 7.8 – 7.12.

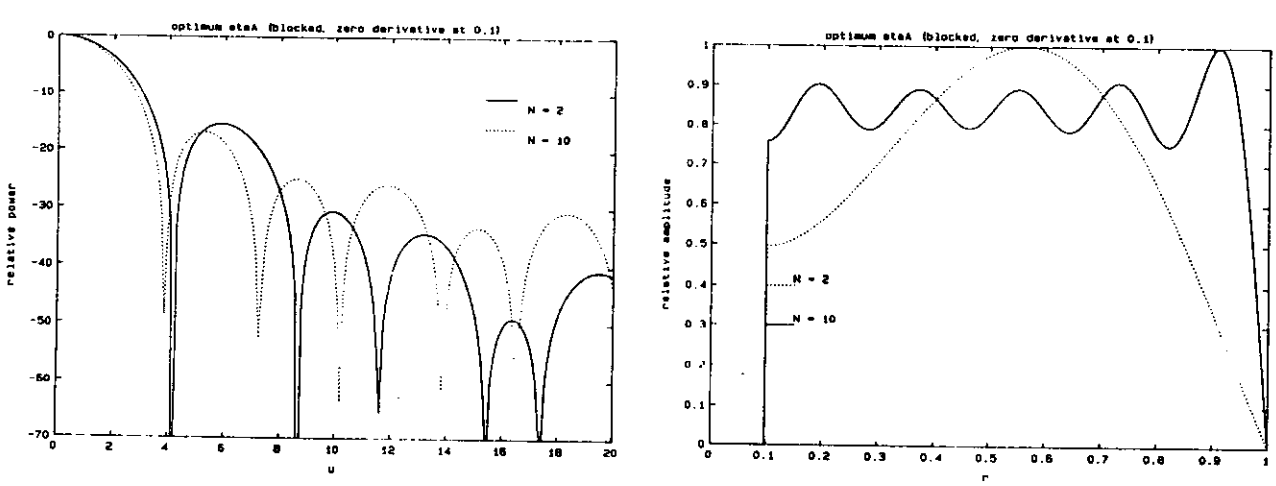

Figure 7.8 g(u) and f(r) for maximum η_a (blocked, zero derivative at $\xi = 0.1$)

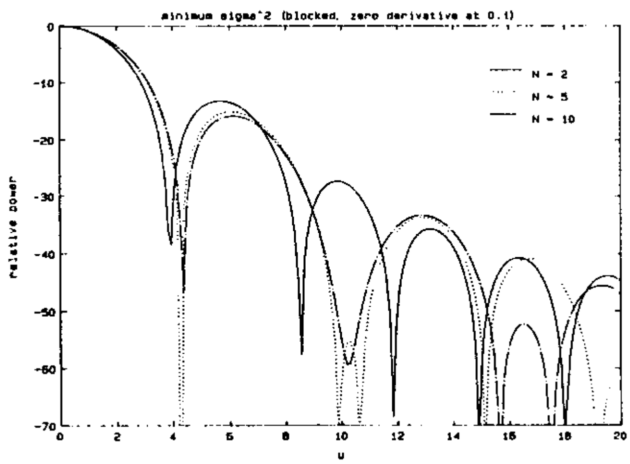

Figure 7.9 g(u) and f(r) for minimum σ^2 (blocked, zero derivative at $\xi = 0.1$)

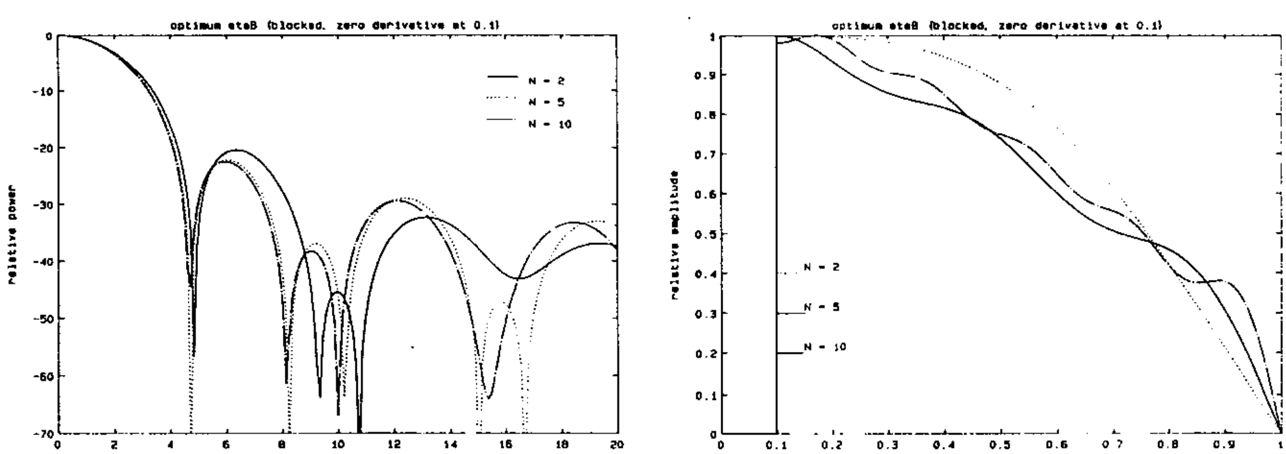

Figure 7.10 g(u) and f(r) for maximum η_b (blocked, zero derivative at $\xi = 0.1$)

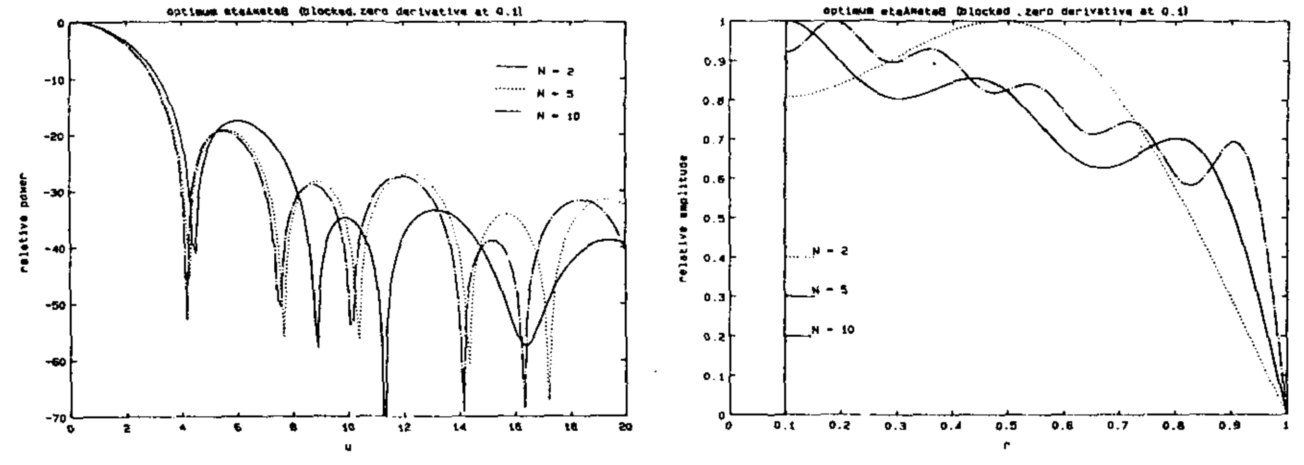

Figure 7.11 g(u) and f(r) for max. $\eta_a \times \eta_b$ (blocked, zero derivative at $\xi = 0.1$)

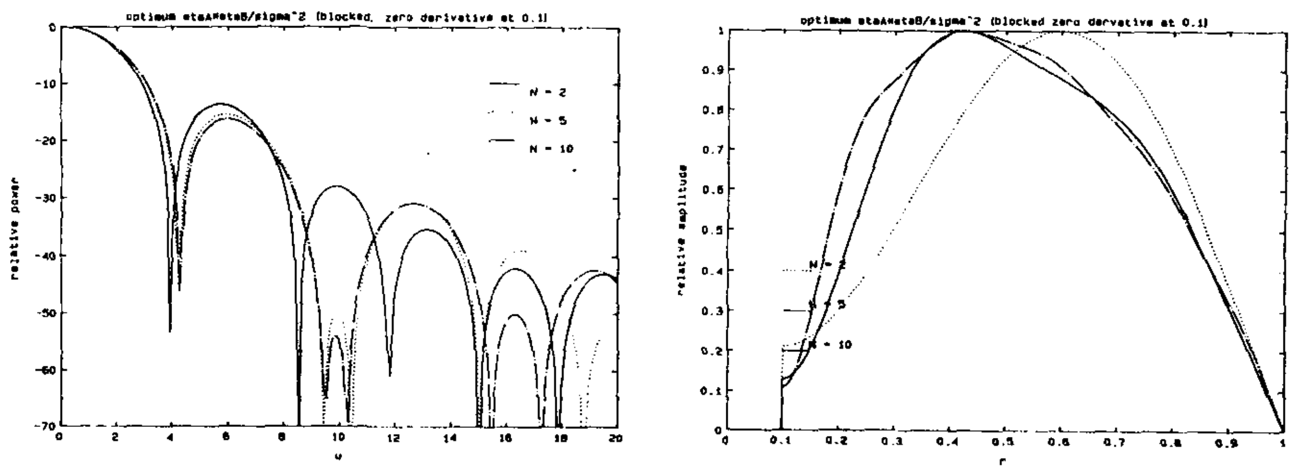

Figure 7.12 g(u) and f(r) for max. $\eta_a \eta_b / \sigma^2$ (blocked, zero derivative at $\xi = 0.1$)

The results of the tables are summarized in figures 7.13 to 7.17.
The following notation is used in the plots:
Xi = 0.1: blocked distribution, zero at $\xi = 0.1$
Xi = 0.05: blocked distribution, zero at $\xi = 0.05$
Xi = 0.1 z.d.: blocked distribution, zero derivative at $\xi = 0.1$
Xi = 0.05 z.d.: blocked distribution, zero derivative at $\xi = 0.05$

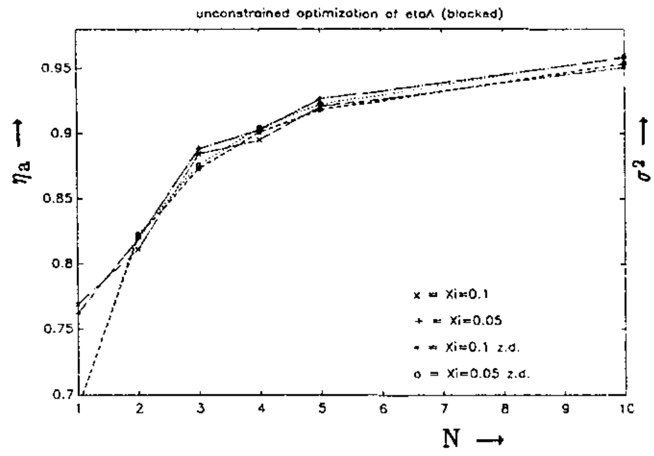

Figure 7.13 The value of η_a against N, where N is the number of elementary functions in the series.

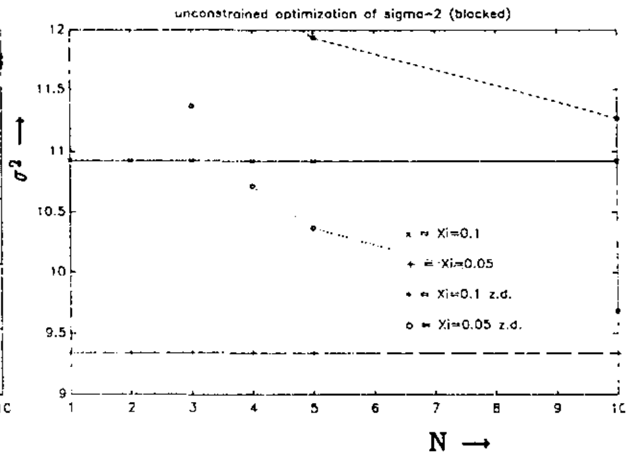

Figure 7.14 The value of σ^2 against N, where N is the number of elementary functions in the series.

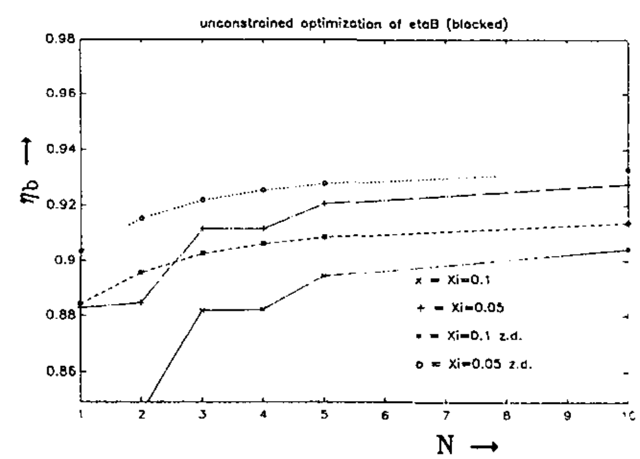

Figure 7.15 The value of η_b against N, where N is the number of elementary functions in the series.

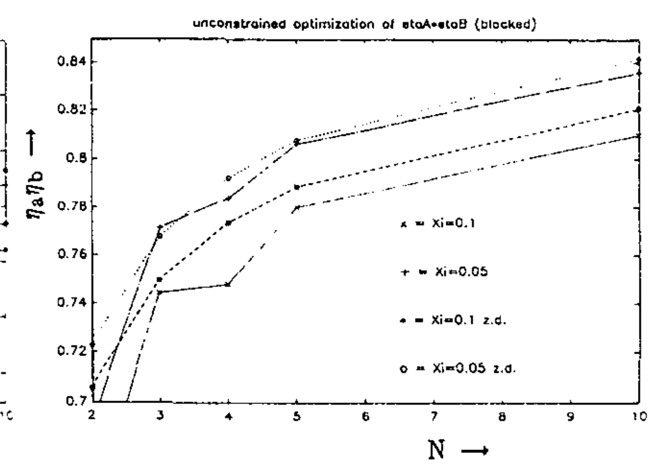

Figure 7.16 The value of $\eta_a\eta_b$ against N, where N is the number of elementary functions in the series.

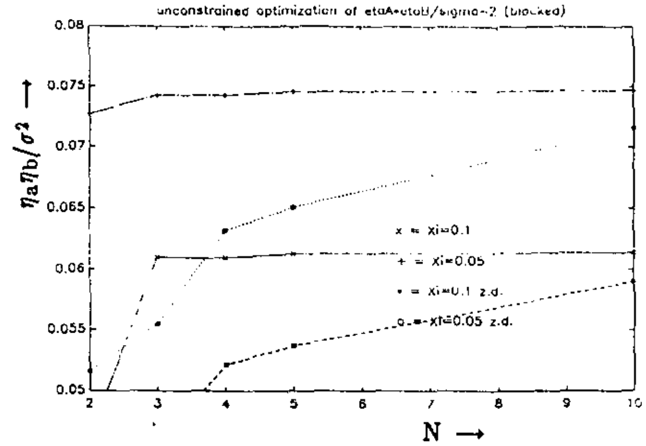

Figure 7.17 The value of $\eta_a\eta_b/\sigma^2$ against N, where N is the number of elementary functions in the series.

Dealing with the values for the blocked case, has to be done with some restraint, if these values are to be compared with those for the unblocked case. For the unblocked case, the lower boundary of the integral (2.5) for the power radiated by the aperture is 0, while for the blocked case it is set on ξ. As the integral of the power radiated by the aperture (2.5) appears in the denominator of the antenna parameters (see (2.7), (2.8) and (2.9)), the optimal values for the blocked aperture have to be taken lower if they are to be compared with unblocked results. This makes it clear that the results for the blocked aperture are always worse than those for the unblocked case. Especially, the value for $\eta_a\eta_b/\sigma^2$ will differ.

8. Conclusions

The method presented in this report makes it possible to optimize two or more antenna parameters simultaneously, with or without constraints. The results obtained with this method agree well with those found in literature. Although the examples given in this report represent only a small set of different pattern requirements, they clearly show the variety of problems that can be handled. Because different source functions were used to optimize η_a, η_b, σ^2, $\eta_a\eta_b$, and $\eta_a\eta_b/\sigma^2$, it is possible to deduce the most suitable source function for optimization of a particular antenna parameter.

An optimal η_a is the prime objective for ground–based antennas in satellite communication systems. An optimal η_b applies to satellite–based antenna systems, because it assures a high amount of power in a prescribed region. Optimization of the product $\eta_a\eta_b/\sigma^2$ will be interesting for ground–based radiometry purposes. As stated a maximum η_b will assure a high amount of power in a prescribed region and a minimal σ^2 will assure a small spread around the axis u=0, thus making the sidelobes low. Including the maximization of η_a will prevent the antenna from becoming too large, thereby reducing the costs of the antenna.

In general, it is true that if an antenna parameter has to be optimized which includes η_b, the Zernike circle polynomials guarantee a good convergence rate.

Comparing the values for the blocked case with those for the unblocked case shows that the results for the blocked aperture are always worse than those for the unblocked case. Especially, the value for $\eta_a\eta_b/\sigma^2$ will differ. So, if a high value for an antenna parameter is needed it will be better to take an unblocked system.

References

[1] Taylor, T.T.
DESIGN OF CIRCULAR APERTURES FOR NARROW BEAMWIDTH AND LOW SIDELOBES.
IRE Trans. Antennas Propag., Vol. AP-8(1960), p. 17-22.

[2] Ishimaru, A. and G. Held
ANALYSIS AND SYNTHESIS OF RADIATION PATTERNS FROM CIRCULAR APERTURES.
Canad. J. Phys., Vol. 38(1960), No. 1, p. 78-99.

[3] Ruze, J.
CIRCULAR APERTURE SYNTHESIS.
IEEE Trans. Antennas Propag., Vol. AP-12(1964), p. 691-694.

[4] Borgiotti, G.
DESIGN OF CIRCULAR APERTURES FOR HIGH BEAM EFFICIENCY AND LOW SIDELOBES.
Alta Frequenza, Vol. 40(1971), p. 652-657.

[5] Mironenko, I.G.
SYNTHESIS OF A FINITE-APERTURE ANTENNA MAXIMIZING THE FRACTION OF POWER RADIATED IN A PRESCRIBED SOLID ANGLE.
Telecommun. Radio Eng. 2, Radio Eng., Vol. 21-22, No. 4 (April 1967), p. 99-104. Transl. of Radiotekhnika (Moscow), Vol. 22, No. 4(April 1967), p. 43-49.

[6] Minkovich, B.M. and V.P. Yakovlev
THEORY OF ANTENNA SYNTHESIS.
Moskva: Sovetskoe Radio Press, 1969.

[7] Yur'yev, A.N.
THEORY OF THE SYNTHESIS OF ANTENNAS HAVING MINIMUM SIDELOBE LEVEL.
Telecommun. Radio Eng. 2, Radio Eng., Vol. 25-26, No. 11(Nov. 1971), p. 117-120. Transl. of Radiotekhnika (Moscow), Vol. 26, No. 11 (Nov. 1971), p. 68-72.

[8] Kouznetsov, V.D.
SIDE LOBE REDUCTION IN CIRCULAR APERTURE ANTENNAS.
In: Proc. Int. Conf. on Antennas and Propagation, London, 28-30 Nov. 1978. Part 1: Antennas.
London: Institution of Electrical Engineers, 1978.
IEE Conference Publication, No. 169. P. 422-427.

[9] Sanzgiri, S.M. and J.K. Butler, R.C. Voges
OPTIMUM APERTURE MONOPULSE EXCITATIONS.
IEEE Trans. Antennas Propag., Vol. AP-20(1972), p. 275-280.

[10] Sanzgiri, S.M. and J.K. Butler
CONSTRAINED OPTIMIZATION OF THE PERFORMANCE INDICES OF ARBITRARY ARRAY ANTENNAS.
IEEE Trans. Antennas Propag., Vol. AP-19(1971), p. 493-498.

[11] Drane, Jr., C. and J. McIlvenna
GAIN MAXIMIZATION AND CONTROLLED NULL PLACEMENT SIMULTANEOUSLY ACHIEVED IN AERIAL ARRAY PATTERNS.
Radio Electron. Eng., Vol. 39(1970), p. 49-57.

[12] Kurth, R.R.
OPTIMIZATION OF ARRAY PERFORMANCE SUBJECT TO MULTIPLE POWER PATTERN CONSTRAINTS.
IEEE Trans. Antennas Propag., Vol. AP-22(1974), p. 103-105.

[13] MICROWAVE ANTENNA THEORY AND DESIGN. Ed. by S. Silver.
New York: McGraw-Hill, 1949.
MIT Radiation Laboratory series, Vol. 12.

[14] Gantmacher, F.R.
THE THEORY OF MATRICES. Vol. 1.
New York: Chelsea, 1959. Transl. from Russian.

[15] Worm, S.C.J.
OPTIMIZATION OF SOME APERTURE ANTENNA PERFORMANCE INDICES WITH AND WITHOUT PATTERN CONSTRAINTS.
Department of Electrical Engineering, Eindhoven University of Technology, Tne Netherlands, 1980.
TH-Report 80-E-112

[16] Watson, G.N.
A TREATISE ON THE THEORY OF BESSEL FUNCTIONS. 2nd ed.
Cambridge University Press, 1960.

[17] Kritskiy, S.V. and M.T. Novosartov
DERIVATION OF THE OPTIMUM FIELD DISTRIBUTIONS FOR ANTENNAS WITH A CIRCULAR APERTURE.
Radio Eng. Electron. Phys., Vol. 19, No. 5(May 1974), p. 23-30. Transl. of Radiotekh. Elektron., Vol. 19, No. 5 (May 1974), p. 955-963.

[18] Taylor, T.T.
DESIGN OF LINE-SOURCE ANTENNAS FOR NARROW BEAMWIDTH AND LOW SIDE LOBES.
IRE Trans. Antennas Propag., Vol. AP-3(1955), p. 16-28.

[19] Slepian, D.
PROLATE SPHEROIDAL WAVE FUNCTIONS, FOURIER ANALYSIS AND UNCERTAINTY - IV: Extensions to many dimensisons; generalized prolate spheroidal functions.
Bell Syst. Tech. J., Vol. 43(1964), p. 3009-3057.

[20] Rhodes, D.R.
ON THE TAYLOR DISTRIBUTION.
IEEE Trans. Antennas Propag., Vol. AP-20(1972), p. 143-145.

[21] Komata, A.
OPTIMUM ILLUMINATION OF CIRCULAR APERTURE FOR LOW NOISE AND NARROW BEAMWIDTH.
In: Summaries of Papers Int. Conf. on Microwaves, Circuit Theory and Information Theory, Tokyo, 7-11 Sept. 1964. Part 1: Microwaves.
Tokyo: Institution of Electrical Communication Engineers of Japan, 1964. P. 361-362.

[22] Ling,C. and E.Lefferts, D. Lee, J. Potenza
RADIATION PATTERN ON PLANAR ANTENNAS WITH OPTIMUM AND ARBITRARY ILLUMINATION.
In: IEEE Int. Conv. Record, New York, 23-26 March 1964, Part 2.
New York: IEEE, 1964. P. 111-124.

[23] Hombach, V.
OPTIMISED APERTURE DISTRIBUTION FOR SATELLITE ANTENNAS WITH MAXIMUM EDGE GAIN.
In: Proc. 6th Int. Conf. on Antennas and Propagation (ICAP 89), Coventry, 4-7 April 1989. Part 1: Antennas.
London: Institution of Electrical Engineers, 1989.
IEE Conference Publication, No. 301. P. 122-125.

[24] Jørgensen, R. and P. Balling
GENERATION OF HIGHLY CONTOURED BEAMS BY SHAPING THE SURFACE OF AN OFFSET-FED SINGLE REFLECTOR.
In: Proc. 11th European Microwave Conf., Amsterdam, 7-11 Sept. 1981.
Sevenoaks, Kent: Microwave Exhibitions and Publishers, 1981.
P. 531-534.

[25] TABLES OF INTEGRAL TRANSFORMS. Vol. 2. Based,in part, on notes left by H. Bateman. Ed. by A. Erdélyi.
New York: McGraw-Hill, 1954. P. 47.
California Institute of Technology Bateman Manuscript Project

[26] Cornbleet, S.
MICROWAVE OPTICS: The optics of microwave antenna design.
London: Academic Press, 1976.

[27] Safak, M. and P.P. Delogne
OPTIMISATION OF CIRCULAR-APERTURE DISTRIBUTIONS FOR INTERFERENCE REDUCTION.
Proc. IEE, Vol. 125(1978), p. 717-723.

[28] Elliott, R.S.
DESIGN OF CIRCULAR APERTURES FOR NARROW BEAMWIDTH AND ASYMMETRIC LOW SIDELOBES.
IEEE Trans. Antennas Propag., Vol. AP-23(1975), p. 523-527.

[29] Sachidananda, M. and S. Ramakrishna
OPTIMUM APERTURE DISTRIBUTIONS IN THE PRESENCE OF BLOCKADE.
Electron. Lett., Vol. 14(1978), p. 556-558.

[30] Galindo-Israel, V. and R. Mittra
A NEW SERIES REPRESENTATION FOR THE RADIATION INTEGRAL WITH APPLICATION TO REFLECTOR ANTENNAS.
IEEE Trans. Antennas Propag., Vol. AP-25(1977), p. 631-641.

[31] Horn, R.A. and C.R. Johnson
MATRIX ANALYSIS.
Cambridge University Press, 1988.

APPENDIX 1 Optimization of multiple antenna parameters

The proof of this theorem can be deduced from the formula for the derivative of a vector–valued function in an N+1–dimensional space.

$$f(\underline{a}+\underline{h}) = f(\underline{a}) + J\underline{h} + \mathcal{O}(\underline{h})$$

where J is the Jacobian matrix.

$$f(\underline{a}+\underline{h}) = \left\{\frac{\underline{a}^T A\underline{a} + 2\underline{h}^T A\underline{a} + \underline{h}^T A\underline{h}}{\underline{a}^T B\underline{a} + 2\underline{h}^T B\underline{a} + \underline{h}^T B\underline{h}}\right\}\left\{\frac{\underline{a}^T C\underline{a} + 2\underline{h}^T C\underline{a} + \underline{h}^T C\underline{h}}{\underline{a}^T D\underline{a} + 2\underline{h}^T D\underline{a} + \underline{h}^T D\underline{h}}\right\}$$

$$= \frac{\underline{a}^T A\underline{a}}{\underline{a}^T B\underline{a}}\left\{\frac{1 + \dfrac{2\underline{h}^T A\underline{a}}{\underline{a}^T A\underline{a}} + \dfrac{\underline{h}^T A\underline{h}}{\underline{a}^T A\underline{a}}}{1 + \dfrac{\underline{a}^T B\underline{a}}{\underline{a}^T B\underline{a}} + \dfrac{\underline{a}^T B\underline{h}}{\underline{a}^T B\underline{a}}}\right\}\frac{\underline{a}^T C\underline{a}}{\underline{a}^T D\underline{a}}\left\{\frac{1 + \dfrac{2\underline{h}^T C\underline{a}}{\underline{a}^T C\underline{a}} + \dfrac{\underline{h}^T C\underline{h}}{\underline{a}^T C\underline{a}}}{1 + \dfrac{\underline{a}^T D\underline{a}}{\underline{a}^T D\underline{a}} + \dfrac{\underline{a}^T D\underline{h}}{\underline{a}^T D\underline{a}}}\right\}$$

$$= \frac{\underline{a}^T A\underline{a}}{\underline{a}^T B\underline{a}}\left\{1+ \frac{2\underline{h}^T A\underline{a}}{\underline{a}^T A\underline{a}} - \frac{2\underline{h}^T B\underline{a}}{\underline{a}^T B\underline{a}} + \mathcal{O}(\underline{h}^2)\right\}\frac{\underline{a}^T C\underline{a}}{\underline{a}^T D\underline{a}}\left\{1+ \frac{2\underline{h}^T C\underline{a}}{\underline{a}^T C\underline{a}} - \frac{2\underline{h}^T D\underline{a}}{\underline{a}^T D\underline{a}} + \mathcal{O}(\underline{h}^2)\right\}$$

neglecting $\mathcal{O}(\underline{h}^2)$ we get:

$$\left\{\frac{\underline{a}^T A\underline{a}}{\underline{a}^T B\underline{a}} + \frac{2}{\underline{a}^T B\underline{a}}\underline{h}^T\left(A\underline{a} - \frac{B\underline{a}\,\underline{a}^T A\underline{a}}{\underline{a}^T B\underline{a}}\right)\right\}\left\{\frac{\underline{a}^T C\underline{a}}{\underline{a}^T D\underline{a}} + \frac{2}{\underline{a}^T D\underline{a}}\underline{h}^T\left(C\underline{a} - \frac{D\underline{a}\,\underline{a}^T C\underline{a}}{\underline{a}^T D\underline{a}}\right)\right\}$$

again neglecting $\mathcal{O}(h^2)$:

$$= \frac{\underline{a}^T A\underline{a}\,\underline{a}^T C\underline{a}}{\underline{a}^T B\underline{a}\,\underline{a}^T D\underline{a}} + 2\underline{h}^T\left\{\frac{1}{\underline{a}^T B\underline{a}}\frac{\underline{a}^T C\underline{a}}{\underline{a}^T D\underline{a}}\left(A\underline{a} - \frac{B\underline{a}\,\underline{a}^T A\underline{a}}{\underline{a}^T B\underline{a}}\right) + \frac{1}{\underline{a}^T D\underline{a}}\frac{\underline{a}^T A\underline{a}}{\underline{a}^T B\underline{a}}\left(C\underline{a} - \frac{D\underline{a}\,\underline{a}^T C\underline{a}}{\underline{a}^T D\underline{a}}\right)\right\}$$

In an extreme is :

$$J\underline{h} = f(\underline{a}+\underline{h}) - f(\underline{a}) = 0$$

$$\Rightarrow \frac{1}{\underline{a}^T B \underline{a}} \frac{\underline{a}^T C \underline{a}}{\underline{a}^T D \underline{a}} (A\underline{a} - \frac{B\underline{a}\,\underline{a}^T A \underline{a}}{\underline{a}^T B \underline{a}}) + \frac{1}{\underline{a}^T D \underline{a}} \frac{\underline{a}^T A \underline{a}}{\underline{a}^T B \underline{a}} (C\underline{a} - \frac{D\underline{a}\,\underline{a}^T C \underline{a}}{\underline{a}^T D \underline{a}}) = 0$$

$$\Rightarrow \left[\frac{1}{\underline{a}^T B \underline{a}} \frac{\underline{a}^T C \underline{a}}{\underline{a}^T D \underline{a}} A + \frac{1}{\underline{a}^T D \underline{a}} \frac{\underline{a}^T A \underline{a}}{\underline{a}^T B \underline{a}} C \right] \underline{a} = \lambda \left[\frac{1}{\underline{a}^T B \underline{a}} B + \frac{1}{\underline{a}^T D \underline{a}} D \right] \underline{a}$$

$$\text{with } \lambda = \frac{\underline{a}^T A \underline{a}}{\underline{a}^T B \underline{a}} \frac{\underline{a}^T C \underline{a}}{\underline{a}^T D \underline{a}}$$

resulting in a generalized eigenvalue problem.

APPENDIX 2 Numerical results (Tables)

Table A1 unconstrained optimization of σ^2 (Bessel with $J_1(\nu_n)=0$)

N	η_a	η_b	σ^2	sll1	sll2	sll3	u3dB
0	1.0000	0.8366	200.317	17.59	23.80	27.94	1.61
1	0.5182	0.8194	7.208	36.59	49.38	60.22	2.41
2	0.5936	0.8666	6.584	26.28	43.82	53.88	2.24
3	0.6258	0.8828	6.323	27.08	34.70	48.94	2.19
4	0.6436	0.8909	6.179	27.29	35.79	40.54	2.13
9	0.6759	0.9041	5.914	27.48	36.37	43.48	2.11
14	0.6905	0.9094	5.960	27.50	36.42	42.57	2.08

Table A2 unconstrained optimization of η_b (Bessel with $J_1(\nu_n)=0$)

N	η_a	η_b	σ^2	sll1	sll2	sll3	u3dB
0	1.0000	0.8366	200.317	17.59	23.80	27.94	1.61
1	0.8706	0.9395	67.773	29.39	29.57	32.87	1.81
2	0.8658	0.9438	52.827	25.91	34.21	34.85	1.86
3	0.8648	0.9446	46.948	25.64	31.95	37.72	1.86
4	0.8646	0.9450	43.792	25.57	31.66	36.03	1.86
9	0.8643	0.9452	38.171	25.52	31.48	35.57	1.86
14	0.8643	0.9452	36.484	25.51	31.48	35.55	1.86

Table A3 unconstrained optimization of $\eta_a\eta_b$ (Bessel with $J_1(\nu_n)=0$)

N	$\eta_a\eta_b$	η_a	η_b	σ^2
0	0.8366	1.0000	0.8366	200.31
1	0.8827	0.9719	0.9083	134.52
2	0.8846	0.9708	0.9112	123.95
3	0.8850	0.9706	0.9118	119.43
4	0.8851	0.9705	0.9120	116.89
9	0.8852	0.9705	0.9121	112.16
14	0.8852	0.9705	0.9122	110.69

Table A4 unconstrained optimization of η_b/σ^2 (Bessel with $J_1(\nu_n)=0$)

N	η_b/σ^2	η_a	η_b	σ^2
2	0.1139	0.5243	0.8228	7.2228
3	0.1320	0.6071	0.8725	6.6052
4	0.1401	0.6412	0.8890	6.3436
5	0.1447	0.6596	0.8970	6.1984
6	0.1476	0.6712	0.9017	6.1060
8	0.1512	0.6847	0.9069	5.9953
10	0.1533	0.6924	0.9097	5.9314

Table A5 unconstrained optimization of $\eta_a\eta_b/\sigma_2$ (Bessel with $J_1(\nu_n)=0$)

N	$\eta_a\eta_b/\sigma^2$	η_a	η_b	σ^2
0	0.0042	1.0000	0.8366	200.317
1	0.0607	0.5413	0.8322	7.421
2	0.0825	0.6395	0.8839	6.855
3	0.0927	0.6801	0.9011	6.608
4	0.0987	0.7018	0.9093	6.466
9	0.1099	0.7392	0.9216	6.194
14	0.1153	0.7547	0.9259	6.066

Table A6 unconstrained optimization of η_a (Bessel with $J_0(\nu_n)=0$)

N	η_a	η_b	σ^2	sll1	sll2	sll3
1	0.6917	0.9098	5.771	27.49	36.41	42.56
2	0.8229	0.8523	9.682	16.06	30.47	37.72
3	0.8763	0.8428	13.610	17.03	21.53	32.84
4	0.9051	0.8396	17.534	17.28	22.88	25.13
5	0.9230	0.8383	21.448	17.38	23.26	26.70
10	0.9605	0.8367	40.799	17.51	23.68	27.69
15	0.9734	0.8365	59.752	17.55	23.75	27.85

Table A7 unconstrained optimization of σ^2 (Bessel with $J_0(\nu_n)=0$)

N	η_a	η_b	σ^2	sll1	sll2	sll3	u3dB
1	0.6917	0.9098	5.7714	27.49	36.41	42.56	2.083
2	0.6923	0.9101	5.7714	27.43	36.38	42.28	2.083
3	0.6926	0.9102	5.7713	27.46	36.31	42.50	2.083
5	0.6928	0.9102	5.7713	27.48	36.37	42.48	2.083
10	0.6930	0.9103	5.7712	27.49	36.43	42.52	2.083
15		0.9103	5.7711	27.49	36.43	42.53	2.083

Table A8 unconstrained optimization of η_b (Bessel with $J_0(\nu_n)=0$)

N	η_a	η_b	σ^2	sll1	sll2	sll3	u3dB
1	0.6917	0.9098	5.771	27.49	36.41	42.56	2.08
2	0.7551	0.9219	6.116	22.69	34.09	40.56	1.97
3	0.7858	0.9283	6.621	24.01	28.36	37.82	1.95
4	0.8032	0.9320	7.169	24.47	29.87	32.12	1.92
5	0.8143	0.9344	7.736	24.70	30.36	33.76	1.92
10	0.8381	0.9395	10.623	25.13	31.04	34.78	1.89
15	0.8466	0.9413	13.492	25.25	31.21	35.23	1.87

Table A9 unconstrained optimization of $\eta_a\eta_b$ (Bessel with $J_0(\nu_n)=0$)

N	$\eta_a\eta_b$	η_a	η_b	σ^2
1	0.6293	0.6916	0.9098	5.771
2	0.7284	0.8071	0.9025	7.532
3	0.7734	0.8557	0.9038	9.528
4	0.7984	0.8821	0.9051	9.051
5	0.8144	0.8987	0.9062	13.637
10	0.8483	0.9335	0.9088	23.918
15	0.8603	0.9455	0.9098	34.026

Table A10 unconstrained optimization of η_b/σ^2 (Bessel with $J_0(\nu_n)=0$)

N	η_b/σ^2	η_a	η_b	σ^2
2	0.1580	0.7047	0.9138	5.782
3	0.1581	0.7073	0.9148	5.784
4	0.1581	0.7081	0.9151	5.785
5	0.1582	0.7085	0.9152	5.785
6	0.1582	0.7087	0.9153	5.786
8	0.1582	0.7089	0.9153	5.786
10	0.1582	0.7090	0.9154	5.786

Table A11 unconstrained optimization of $\eta_a\eta_b/\sigma^2$ (Bessel with $J_0(\nu_n)=0$)

N	$\eta_a\eta_b/\sigma^2$	η_a	η_b	σ^2
1	0.1090	0.6917	0.9099	5.7714
2	0.1144	0.7406	0.9211	5.9614
3	0.1155	0.7509	0.9245	6.0089
4	0.1159	0.7541	0.9256	6.0254
5	0.1160	0.7555	0.9261	6.0313
10	0.1162	0.7571	0.9267	6.0381
15	0.1162	0.7573	0.9268	6.0381

Table A12 unconstrained optimization of σ^2 (Zernike)

N	η_a	η_b	σ^2	sll1	sll2	sll3
1	0.7537	0.9261	5.9606	24.62	33.57	39.73
2	0.6968	0.9116	5.7423	27.32	36.53	42.79
3	0.6966	0.9116	5.7421	27.43	36.54	42.75
4	0.6966	0.9116	5.7417	27.50	36.53	42.59
5	0.6966	0.9116	5.7412	27.49	36.48	42.34
10	0.6972	0.9118	5.7371	27.49	36.42	42.56

Table A13 unconstrained optimization of η_b (Zernike)

N	η_a	η_b	σ^2	sll1	sll2	sll3
1	0.8671	0.9432	22.708	23.49	31.27	36.22
2	0.8642	0.9451	35.373	25.45	31.68	35.65
3	0.8642	0.9451	34.321	25.51	31.47	35.53
4	0.8642	0.9451	34.362	25.51	31.47	35.54
5	0.8642	0.9451	34.361	25.51	31.47	35.54
10	0.8642	0.9451	34.361	25.51	31.47	35.54

Table A14 unconstrained optimization of $\eta_a\eta_b$ (Zernike)

N	$\eta_a\eta_b$	η_a	η_b	σ^2
1	0.8587	0.9709	0.9109	97.747
2	0.8851	0.9704	0.9121	101.593
3	0.8851	0.9704	0.9121	108.759
4	0.8851	0.9704	0.9121	108.791
5	0.8851	0.9704	0.9121	108.790
10	0.8851	0.9704	0.9121	108.790

Table A15 unconstrained optimization of η_b/σ^2 (Zernike)

N	η_b/σ^2	η_a	η_b	σ^2
3	0.1592	0.7127	0.9166	5.756
4	0.1592	0.7126	0.9166	5.756
5	0.1592	0.7127	0.9166	5.756
6	0.1592	0.7127	0.9166	5.755
8	0.1593	0.7129	0.9167	5.754
10	0.1593	0.7131	0.9168	5.752

Table A16 unconstrained optimization of $\eta_a\eta_b/\sigma^2$ (Zernike)

N	$\eta_a\eta_b/\sigma^2$	η_a	η_b	σ^2
1	0.1175	0.7582	0.9273	5.9819
2	0.1175	0.7612	0.9278	6.0081
3	0.1176	0.7613	0.9278	6.0084
4	0.1176	0.7613	0.9278	6.0079
5	0.1176	0.7614	0.9278	6.0073
10	0.1178	0.7619	0.9280	6.0028

Table A17 unconstrained optimization of $\sigma^2\,(1-r^2)^N$

N	η_a	η_b	σ^2	sll1	sll2	sll3
1	0.7537	0.9261	5.9606	24.62	33.57	39.73
2	0.6968	0.9116	5.7423	27.32	36.53	42.79
3	0.6966	0.9115	5.7421	27.43	36.54	42.75
4	0.6966	0.9115	5.7417	27.50	36.27	42.59
5	0.6967	0.9116	5.7412	27.49	36.48	42.34

Table A18 unconstrained optimization of $\eta_b\,(1-r^2)^N$

N	η_a	η_b	σ^2	sll1	sll2	sll3
1	0.8642	0.9451	35.373	25.45	31.68	35.65
2	0.8642	0.9451	34.320	25.51	31.48	35.53
3	0.8642	0.9451	34.361	25.51	31.48	35.53
4	0.8642	0.9451	34.361	25.51	31.47	35.54
5	0.8642	0.9451	34.361	25.51	31.47	35.54

Table A19 unconstrained optimization of $\eta_a \eta_b \, (1-r^2)^N$

N	$\eta_a\eta_b$	η_a	η_b	σ^2
1	0.8787	0.9873	0.8900	129.38
2	0.8839	0.9704	0.9109	109.59
3	0.8851	0.9704	0.9121	108.75
4	0.8851	0.9704	0.9121	108.79
5	0.8851	0.9704	0.9121	108.79

Table A20 unconstrained optimization of $\eta_b/\sigma^2 \, (1-r^2)^N$

N	η_b/σ^2	η_a	η_b	σ^2
2	0.1537	0.7127	0.9166	5.961
3	0.1592	0.7127	0.9166	5.756
4	0.1592	0.7126	0.9166	5.756
5	0.1592	0.7127	0.9166	5.756
6	0.1592	0.7127	0.9166	5.755

Table A21 unconstrained optimization of $\eta_a\eta_b/\sigma^2\ (1-r^2)^N$

N	$\eta_a\eta_b/\sigma^2$	η_a	η_b	σ^2
1	0.1175	0.7582	0.9273	5.9819
2	0.1175	0.7612	0.9278	6.0081
3	0.1176	0.7613	0.9278	6.0084
4	0.1176	0.7613	0.9278	6.0079
5	0.1176	0.7614	0.9278	6.0073

Table A22 unconstrained optimization of η_a ($\xi = 0.1$)

N	η_a	η_b	σ^2	sll1	sll2	sll3	u3dB
1	0.7688	0.8408	10.9234	16.18	33.15	57.26	1.86
2	0.8112	0.7734	12.8040	13.89	29.59	33.61	1.75
3	0.8844	0.8075	20.5250	16.09	24.46	23.59	1.70
4	0.8950	0.7962	22.5409	15.80	26.16	22.92	1.67
5	0.9207	0.8081	30.1596	16.37	25.32	24.88	1.65
10	0.9507	0.8093	51.1978	16.53	25.49	25.45	1.64

Table A23 unconstrained optimization of σ^2 ($\xi = 0.1$)

N	η_a	η_b	σ^2	sll1	sll2	sll3	u3dB
1	0.7688	0.8408	10.9234	16.18	33.15	57.26	1.86
2	0.7686	0.8409	10.9234	16.18	33.15	57.30	1.86
3	0.7695	0.8415	10.9231	16.21	33.03	57.21	1.86
4	0.7695	0.8415	10.9231	16.21	33.03	57.30	1.86
5	0.7698	0.8417	10.9228	16.21	33.08	57.88	1.86
10	0.7700	0.8419	10.9222	16.22	33.10	57.90	1.86

Table A24 unconstrained optimization of η_b ($\xi = 0.1$)

N	η_a	η_b	σ^2	sll1	sll2	sll3	u3dB
1	0.7688	0.8408	10.9234	16.18	33.15	57.26	1.86
2	0.7331	0.8463	11.1786	16.95	32.89	44.87	1.93
3	0.8008	0.8817	14.9648	20.07	24.81	39.84	1.86
4	0.7950	0.8822	15.0692	20.12	25.00	40.16	1.86
5	0.8190	0.8943	18.8336	21.02	49.10	27.06	1.86
10	0.8343	0.9043	26.4640	21.75	43.11	28.28	1.86

Table A25 unconstrained optimization of $\eta_a\eta_b$ ($\xi = 0.1$)

N	$\eta_a\eta_b$	η_a	η_b	σ^2
2	0.6547	0.7933	0.8254	11.1653
3	0.7445	0.8654	0.8604	17.0700
4	0.7478	0.8726	0.8570	17.4611
5	0.7803	0.8980	0.8690	23.3086
10	0.8102	0.9251	0.8759	36.0890

Table A26 unconstrained optimization of $\eta_a\eta_b/\sigma^2$ ($\xi = 0.1$)

N	$\eta_a\eta_b/\sigma^2$	η_a	η_b	σ^2
2	0.0463	0.7790	0.8363	10.9569
3	0.0610	0.8010	0.8515	11.1764
4	0.0610	0.8019	0.8513	11.1814
5	0.0613	0.8053	0.8536	11.2153
10	0.0614	0.8070	0.8545	11.2297

Table A27 unconstrained optimization of η_a ($\xi = 0.05$)

N	η_a	η_b	σ^2	sll1	sll2	sll3	u3dB
1	0.7618	0.9335	9.3359	18.36	33.49	42.04	1.90
2	0.8194	0.8077	11.5774	14.71	30.17	34.36	1.76
3	0.8883	0.8311	17.9673	16.83	22.75	25.61	1.73
4	0.9026	0.8200	20.3840	16.58	24.50	23.63	1.69
5	0.9265	0.8283	26.6477	17.06	23.96	26.18	1.67
10	0.9581	0.8272	46.2287	17.16	24.31	26.73	1.64

Table A28 unconstrained optimization of σ^2 ($\xi = 0.05$)

N	η_a	η_b	σ^2	sll1	sll2	sll3	u3dB
1	0.7618	0.8827	9.3359	18.36	33.49	42.04	1.90
2	0.7615	0.8827	9.3359	18.37	33.49	42.03	1.94
3	0.7623	0.8833	9.3356	18.39	33.39	41.98	1.93
4	0.7623	0.8833	9.3356	18.39	33.40	41.98	1.92
5	0.7626	0.8835	9.3353	18.40	33.46	41.83	1.92
10	0.7626	0.8836	9.3348	18.41	33.49	41.95	1.92

Table A29 unconstrained optimization of η_b ($\xi = 0.05$)

N	η_a	η_b	σ^2	sll1	sll2	sll3	u3dB
1	0.7618	0.8827	9.3359	18.36	33.49	42.04	1.90
2	0.7402	0.8845	9.4062	19.04	33.31	41.85	1.97
3	0.8003	0.9116	11.9064	22.35	35.59	27.18	1.93
4	0.7990	0.9116	11.9085	22.36	35.27	27.28	1.92
5	0.8201	0.9207	14.3787	23.20	34.41	30.28	1.92
10	0.8371	0.9278	19.2025	23.83	33.80	31.74	1.92

Table A30 unconstrained optimization of $\eta_a\eta_b$ ($\xi = 0.05$)

N	$\eta_a\eta_b$	η_a	η_b	σ^2
2	0.6911	0.8012	0.8626	9.7866
3	0.7714	0.8682	0.8885	14.2926
4	0.6842	0.8794	0.8848	14.9784
5	0.8065	0.9027	0.8935	19.4142
10	0.8361	0.9314	0.8977	30.3315

Table A31 unconstrained optimization of $\eta_a\eta_b/\sigma^2$($\xi = 0.05$)

N	$\eta_a\eta_b/\sigma^2$	η_a	η_b	σ^2
2	0.0727	0.7785	0.8780	9.3964
3	0.0743	0.7978	0.8901	9.5530
4	0.0743	0.7992	0.8900	9.5611
5	0.0746	0.8021	0.8918	9.5845
10	0.0747	0.8038	0.8926	9.5958

Table A32 unconstrained optimization η_a ($\xi = 0.1$, z.d.)

N	η_a	η_b	σ^2	sll1	sll2	sll3	u3dB
1	0.6906	0.8842	76.5289	23.29	31.59	35.63	2.02
2	0.8206	0.8279	19.8492	15.33	30.58	34.42	1.78
3	0.8729	0.8214	52.7631	16.39	22.53	27.64	1.73
4	0.9009	0.8186	53.3849	16.54	24.41	23.76	1.69
5	0.9181	0.8179	54.5004	16.67	24.50	25.47	1.66
10	0.9536	0.8170	62.3075	16.79	24.97	26.00	1.64

Table A33 unconstrained optimization σ^2 ($\xi = 0.1$, z.d)

N	η_a	η_b	σ^2	sll1	sll2	sll3	u3dB
1	0.6906	0.8842	76.5289	23.29	31.59	35.63	2.02
2	0.7998	0.7399	14.4403	13.21	27.41	35.75	1.72
3	0.7491	0.7698	12.9291	13.96	34.89	45.70	1.80
4	0.7732	0.8016	12.2598	14.84	36.46	38.37	1.81
5	0.7670	0.8100	11.9371	15.10	33.78	40.88	1.81
10	0.7720	0.8329	11.2662	15.86	33.37	52.32	1.81

Table A34 unconstrained optimization η_b($\xi = 0.1$, z.d)

N	η_a	η_b	σ^2	sll1	sll2	sll3	u3dB
1	0.6906	0.8841	76.5289	23.29	31.59	35.63	2.02
2	0.7527	0.8954	55.1277	20.47	45.40	32.37	1.97
3	0.7847	0.9026	72.1146	21.70	33.28	29.73	1.90
4	0.8018	0.9062	59.0666	21.97	36.57	27.74	1.89
5	0.8130	0.9087	70.5527	22.19	36.97	28.97	1.87
10	0.8361	0.9137	65.9799	22.52	38.30	29.46	1.86

Table A35 unconstrained optimization of $\eta_a\eta_b$ ($\xi = 0.1$, z.d.)

N	$\eta_a\eta_b$	η_a	η_b	σ^2
2	0.7054	0.8048	0.8765	32.9712
3	0.7498	0.8529	0.8792	61.3762
4	0.7736	0.8786	0.8806	41.4220
5	0.7890	0.8946	0.8820	60.3350
10	0.8208	0.9277	0.8848	59.2650

Table A36 unconstrained optimization of $\eta_a\eta_b/\sigma^2$ (ξ = 0.1, z.d.)

N	$\eta_a\eta_b/\sigma^2$	η_a	η_b	σ^2
2	0.0418	0.8081	0.7623	14.7149
3	0.0455	0.7705	0.7786	13.1680
4	0.0522	0.8055	0.8174	12.5984
5	0.0537	0.7991	0.8232	12.2475
10	0.0590	0.8081	0.8467	11.5854

Table A37 unconstrained optimization η_a (ξ = 0.05, z.d)–1

N	η_a	η_b	σ^2	sll1	sll2	sll3	u3dB
1	0.6915	0.9034	43.0743	26.17	40.56	37.63	2.08
2	0.8226	0.8459	13.9792	15.86	30.46	36.46	1.81
3	0.8759	0.8373	34.8215	16.87	21.76	30.94	1.75
4	0.9045	0.8342	23.8801	17.08	23.29	24.67	1.70
5	0.9223	0.8330	34.8215	17.19	23.57	26.38	1.69
10	0.9592	0.8316	50.3044	17.32	24.01	27.17	1.64

Table A38 unconstrained optimization σ^2 (ξ = 0.05, z.d.)

N	η_a	η_b	σ^2	sll1	sll2	sll3	u3dB
1	0.6915	0.9034	43.0743	26.17	40.56	37.63	2.08
2	0.8148	0.7945	12.7625	14.38	29.20	36.21	1.75
3	0.7538	0.8179	11.3600	15.28	40.11	42.77	1.86
4	0.7749	0.8475	10.7161	16.43	34.18	41.35	1.86
5	0.7647	0.8548	10.3654	16.79	32.51	48.04	1.89
10	0.7659	0.8755	9.6842	17.86	33.26	42.25	1.90

Table A39 unconstrained optimization of η_b (ξ = 0.05, z.d.)1

N	η_a	η_b	σ^2	sll1	sll2	sll3	u3dB
1	0.6915	0.9034	43.0743	26.17	40.56	37.63	2.08
2	0.7546	0.9152	31.1951	22.05	36.04	37.25	1.97
3	0.7854	0.9218	40.9612	23.36	29.43	34.56	1.93
4	0.8031	0.9255	33.2388	23.76	31.27	30.58	1.92
5	0.8143	0.9279	40.4678	24.05	31.72	32.13	1.90
10	0.8380	0.9330	38.2808	24.38	32.49	33.02	1.86

Table A40 unconstrained optimization of $\eta_a\eta_b$ (ξ = 0.05, z.d.)

N	$\eta_a\eta_b$	η_a	η_b	σ^2
2	0.7228	0.8068	0.8959	19.8132
3	0.7677	0.8553	0.8976	37.1679
4	0.7924	0.8816	0.8989	25.7521
5	0.8082	0.8981	0.9000	38.2833
10	0.8417	0.9325	0.9027	40.7880

Table A41 unconstrained optimization of $\eta_a\eta_b/\sigma^2$ (ξ = 0.05, z.d.)

N	$\eta_a\eta_b/\sigma^2$	η_a	η_b	σ^2
2	0.0516	0.8198	0.8168	12.9610
3	0.0555	0.7794	0.8268	11.5912
4	0.0632	0.8090	0.8602	10.9973
5	0.0651	0.8004	0.8649	10.6324
10	0.0716	0.8059	0.8854	9.9553

ISSN 0167-9708
Coden: TEUEDE

(222) Jóźwiak, L.
THE FULL-DECOMPOSITION OF SEQUENTIAL MACHINES WITH THE SEPARATE REALIZATION OF THE NEXT-STATE AND OUTPUT FUNCTIONS.
EUT Report 89-E-222. 1989. ISBN 90-6144-222-2

(223) Jóźwiak, L.
THE BIT FULL-DECOMPOSITION OF SEQUENTIAL MACHINES.
EUT Report 89-E-223. 1989. ISBN 90-6144-223-0

(224) Book of abstracts of the first Benelux-Japan Workshop on Information and Communication Theory, Eindhoven, The Netherlands, 3-5 September 1989.
Ed. by Han Vinck.
EUT Report 89-E-224. 1989. ISBN 90-6144-224-9

(225) Hoeijmakers, M.J.
A POSSIBILITY TO INCORPORATE SATURATION IN THE SIMPLE, GLOBAL MODEL OF A SYNCHRONOUS MACHINE WITH RECTIFIER.
EUT Report 89-E-225. 1989. ISBN 90-6144-225-7

(226) Dahiya, R.P. and E.M. van Veldhuizen, W.R. Rutgers, L.H.Th. Rietjens
EXPERIMENTS ON INITIAL BEHAVIOUR OF CORONA GENERATED WITH ELECTRICAL PULSES SUPERIMPOSED ON DC BIAS.
EUT Report 89-E-226. 1989. ISBN 90-6144-226-5

(227) Bastings, R.H.A.
TOWARD THE DEVELOPMENT OF AN INTELLIGENT ALARM SYSTEM IN ANESTHESIA.
EUT Report 89-E-227. 1989. ISBN 90-6144-227-3

(228) Hekker, J.J.
COMPUTER ANIMATED GRAPHICS AS A TEACHING TOOL FOR THE ANESTHESIA MACHINE SIMULATOR.
EUT Report 89-E-228. 1989. ISBN 90-6144-228-1

(229) Oostrom, J.H.M. van
INTELLIGENT ALARMS IN ANESTHESIA: An implementation.
EUT Report 89-E-229. 1989. ISBN 90-6144-229-X

(230) Winter, M.R.M.
DESIGN OF A UNIVERSAL PROTOCOL SUBSYSTEM ARCHITECTURE: Specification of functions and services.
EUT Report 89-E-230. 1989. ISBN 90-6144-230-3

(231) Schemmann, M.F.C. and H.C. Heyker, J.J.M. Kwaspen, Th.G. van de Roer
MOUNTING AND DC TO 18 GHz CHARACTERISATION OF DOUBLE BARRIER RESONANT TUNNELING DEVICES.
EUT Report 89-E-231. 1989. ISBN 90-6144-231-1

(232) Sarma, A.D. and M.H.A.J. Herben
DATA ACQUISITION AND SIGNAL PROCESSING/ANALYSIS OF SCINTILLATION EVENTS FOR THE OLYMPUS PROPAGATION EXPERIMENT.
EUT Report 89-E-232. 1989. ISBN 90-6144-232-X

(233) Nederstigt, J.A.
DESIGN AND IMPLEMENTATION OF A SECOND PROTOTYPE OF THE INTELLIGENT ALARM SYSTEM IN ANESTHESIA.
EUT Report 90-E-233. 1990. ISBN 90-6144-233-8

(234) Philippens, E.H.J.
DESIGNING DEBUGGING TOOLS FOR SIMPLEXYS EXPERT SYSTEMS.
EUT Report 90-E-234. 1990. ISBN 90-6144-234-6

(235) Heffels, J.J.M.
A PATIENT SIMULATOR FOR ANESTHESIA TRAINING: A mechanical lung model and a physiological software model.
EUT Report 90-E-235. 1990. ISBN 90-6144-235-4

(236) Lammers, J.O.
KNOWLEDGE BASED ADAPTIVE BLOOD PRESSURE CONTROL: A Simplexys expert system application.
EUT Report 90-E-236. 1990. ISBN 90-6144-236-2

(237) Ren Qingchang
PREDICTION ERROR METHOD FOR IDENTIFICATION OF A HEAT EXCHANGER.
EUT Report 90-E-237. 1990. ISBN 90-6144-237-0

ISSN 0167-9708
Coden: TEUEDE

(238) Lammers, J.O.
THE USE OF PETRI NET THEORY FOR SIMPLEXYS EXPERT SYSTEMS PROTOCOL CHECKING.
EUT Report 90-E-238. 1990. ISBN 90-6144-238-9

(239) Wang, X.
PRELIMINARY INVESTIGATIONS ON TACTILE PERCEPTION OF GRAPHICAL PATTERNS.
EUT Report 90-E-239. 1990. ISBN 90-6144-239-7

(240) Lutgens, J.M.A.
KNOWLEDGE BASE CORRECTNESS CHECKING FOR SIMPLEXYS EXPERT SYSTEMS.
EUT Eeport 90-E-240. 1990. ISBN 90-6144-240-0

(241) Brinker, A.C. den
A MEMBRANE MODEL FOR SPATIOTEMPORAL COUPLING.
EUT Report 90-E-241. 1990. ISBN 90-6144-241-9

(242) Demarteau, J.I.M. and H.C. Heyker, J.J.M. Kwaspen, Th.G. van de Roer
MICROWAVE NOISE MEASUREMENTS ON DOUBLE BARRIER RESONANT TUNNELING DIODES.
EUT Report 90-E-242. 1990. ISBN 90-6144-242-7

(243) Massee, P. and H.A.L.M. de Graaf, W.J.M. Balemans, H.G. Knoopers, H.H.J. ten Kate
PREDESIGN OF AN EXPERIMENTAL (5-10 MWt) DISK MHD FACILITY AND PROSPECTS OF COMMERCIAL (1000 MWt) MHD/STEAM SYSTEMS.
EUT Report 90-E-243. 1990. ISBN 90-6144-243-5

(244) Klompstra, Martin and Ton van den Boom, Ad Damen
A COMPARISON OF CLASSICAL AND MODERN CONTROLLER DESIGN: A case study.
EUT Report 90-E-244. 1990. ISBN 90-6144-244-3

(245) Berg, P.H.G. van de
ON THE ACCURACY OF RADIOWAVE PROPAGATION MEASUREMENTS: Olympus propagation experiment.
EUT Report 90-E-245. 1990. ISBN 90-6144-245-1